Pharmacological Research 223 (2026) 108072

Contents lists available at ScienceDirect

Pharmacological Research

journal homepage: www.elsevier.com/locate/yphrs

Functional, synaptoproteomic and structural adaptations underlying sex-dependent traumatic stress susceptibility/resilience in the hippocampus

Sebastiano A. Torrisi [a,b,1], Maria Rosaria Tropea [a,b,1], Silvia Rizzo [a], Mattia Giovenzana [c,d], Chiara Magri [e], Alessandro Barbon [e], Jessica Mingardi [d,f], Clizia Chinello [d], Lisa Pagani [d], Isabella Piga [d], Loredana Leggio [a], Nunzio Iraci [a], Walter Gulisano [a], Filippo Drago [a], Daniela Puzzo [a,b], Laura Musazzi [d,g,2], Gian Marco Leggio [a,2,*]

[a] Department of Biomedical and Biotechnological Sciences, University of Catania, Catania, Italy
[b] Oasi Research Institute - IRCCS, Troina, EN, Italy
[c] PhD Program in Neuroscience, University of Milano-Bicocca, Monza, (MB), Italy
[d] School of Medicine and Surgery, University of Milano-Bicocca, Monza, Italy
[e] Department of Molecular and Translational Medicine, University of Brescia, Brescia 25121, Italy
[f] Department of Medical Biotechnology and Translational Medicine, University of Milan, Milan, Italy
[g] Fondazione IRCCS San Gerardo dei Tintori, Monza, Italy

ARTICLE INFO

Keywords:
PTSD
Resilience
Susceptibility
hippocampus
Animal model
Biological sex

ABSTRACT

Although post-traumatic stress disorder (PTSD) occurs more in women than in men, how sex influences trauma susceptibility remains largely unknown. We developed the arousal-based individual screening (AIS) model, which identifies mice as susceptible/resilient to PTSD-like phenotypes, based on changes in startle reactivity induced by 24-hour-restraint. To test the hypothesis that sex drives trauma susceptibility/resilience, we applied a multidisciplinary approach involving electrophysiological, structural, and synaptoproteomic analyses of the hippocampus in susceptible and resilient mice of both sexes. Female mice were more susceptible to the trauma than male mice and exhibited long-lasting PTSD-like phenotypes. Long-term potentiation (LTP) was impaired in hippocampal slices of both male and female susceptible mice, whereas short-term presynaptic forms of plasticity and vesicle recycling remained unchanged. Increased apical dendritic length and augmented basal dendritic spine density of pyramidal neurons were found in CA1 of male susceptible mice, while decreased dendritic length of granule neurons was uncovered in the dentate gyrus of female resilient mice. Although minor synaptoproteomic changes were observed, bioinformatic analysis suggested sex- and susceptibility/resilience-dependent profiles. Notably, several pathways involving RHO Family GTPases were found to be upregulated exclusively in susceptible male mice. Accordingly, the Rac1/Rac3 GTPases inhibitor EHop-016 rescued the hippocampal LTP impairment in susceptible male mice but not in susceptible female mice. Our findings suggest that the AIS model mirrors sex differences in PTSD susceptibility/resilience highlighting associated functional, molecular and structural alterations. This model may represent a critical first step for studying sex-dependent pathophysiological mechanisms subserving PTSD susceptibility and for sex-tailored drug development.

1. Introduction

Post-traumatic stress disorder (PTSD) is a severe neuropsychiatric disorder that occurs in vulnerable individuals, in the months and years following exposure to trauma [1]. Individuals with PTSD experience multiple symptoms belonging to four symptom clusters: intrusion symptoms, avoidance symptoms, alterations in mood/cognition and hyperarousal symptoms [2]. From a therapeutic perspective, the most used treatments for PTSD are psychological therapies that can be both trauma-focused (prolonged exposure and cognitive processing therapy)

* Correspondence to: Department of Biomedical and Biotechnological Sciences, Elininate Catania University of Catania, Via Santa Sofia 97, Catania 95123, Italy.
E-mail address: gianmarco.leggio@unict.it (G.M. Leggio).
[1] Shared first authorship
[2] Shared last authorship

https://doi.org/10.1016/j.phrs.2025.108072
Received 18 October 2025; Received in revised form 20 November 2025; Accepted 16 December 2025
Available online 24 December 2025

and non-trauma-focused interventions [3]. At the pharmacological level, chronic treatments with the selective serotonin reuptake inhibitors such as paroxetine and sertraline (the only antidepressants approved by the Food and Drug Administration for the treatment of PTSD) are recommended [4]. However, these therapeutic treatments are effective only in a small percentage of individuals with PTSD [5]. Thus, there is an urgent need to understand the pathophysiological mechanisms subserving PTSD, paving the way for identification of novel pharmacological targets.

Multiple epidemiological studies report that women are approximately twice as likely as men to receive a diagnosis of PTSD and exhibit greater symptom chronicity/severity compared with men [6–8]. The observation of these evident clinical sex differences in PTSD is not simply an epidemiological finding; it points to fundamental biological distinctions that necessitate investigation at a neurobiological level. The neurobiological basis for this sex discrepancy in PTSD outcomes is complex and may arise from multiple interactions between biological and non-biological factors [9]. In spite of this unquestionable sex difference in PTSD outcomes, the vast majority of preclinical studies in the field have been paradoxically carried out using exclusively male rodents [10]. The limited number of studies performed using female rodents have led to controversial findings and have basically failed in modelling the human condition, in which being female represents a risk factor for the development of PTSD [11,12]. Thus, translational models useful to study sex differences in PTSD susceptibility and resilience are needed.

We have recently developed the arousal based-individual screening (AIS) model, which is a mouse model useful for the study of PTSD [13]. The AIS model combines the traumatization (24-hour-restraint; [14]) of C57BL/6 J mice with a novel individual screening consisting of z-normalization of post-trauma changes in startle reactivity. The AIS model has the advantage of modelling the chronicity of multiple PTSD symptoms. Indeed, with this model we can identify susceptible male mice exhibiting multiple PTSD-like phenotypes (exaggerated startle reactivity, exaggerated fear responses to a trauma-related cue, social/-cognitive impairment), resembling different PTSD symptoms, up to 75 days post-trauma. The AIS model has already allowed us to explore different pathophysiological aspects, including epigenetic mechanisms [15] and alterations of the gut-brain axis [16], which may play a key role in traumatic stress susceptibility/resilience. However, our previous studies have been performed only in male mice.

Preclinical research and functional neuroimaging studies have led to the identification of key brain regions in PTSD etiopathogenesis [17]. Among these, the hippocampus has been shown to be involved in explicit memory processes and in the encoding of context during fear conditioning [18,19]. Indeed, neural projections from the anterior cingulate cortex to the ventral hippocampus mediate contextual fear generalization [18], while the connection of ventral hippocampus with amygdala regulates the encoding of emotional memories [20]. Accordingly, multiple findings suggest that an impairment of hippocampal synaptic plasticity may be crucial in the pathophysiology of PTSD [13,21,22].

In the present study we hypothesized that sex drives distinct mechanisms underlying trauma susceptibility/resilience in the hippocampus. To test this hypothesis, we firstly assessed the effectiveness of the AIS model in female mice. We then combined the AIS model with integrated electrophysiological, structural, and synaptoproteomic approaches to identify sex-dependent mechanisms of traumatic stress susceptibility/resilience in the hippocampus, with the objective of identifying potential sex-tailored therapeutic targets.

2. Materials and methods

2.1. Chemicals and reagents

N4-(9-Ethyl-9H-carbazol-3-yl)-N2-[3-(4-morpholinyl)propyl]-2,4-pyrimidinediamine(EHop-016) was purchased from MedChemExpress (MCE). EHop-016 exhibits a remarkable potency, with an IC50 of approximately 1.1 μM for Rac1/3 inhibition [23]. For this reason, EHop-016 is significantly more potent (100-fold greater) than its analog NSC23766, and 10–50 times more effective than other currently available Rac GTPase inhibitors [23]. We selected a concentration of 3 μM to achieve a maximal inhibition and to maintain selectivity for Rac1 and Rac3 GTPases, given that EHop-016 is highly selective for Rac1 and Rac3 GTPases at concentrations of 5 μM or less [23]. Toluidine Blue was purchased from (Sigma-Aldrich, St. Louis, MO, United States). (2 R)-amino-5-phosphonovaleric acid (APV) was obtained from Sigma-Aldrich. NaCl, KCl, Na_2HPO_4, $NaHCO_3$, $CaCl_2$, $MgCl_2$ and glucose were obtained from Sigma-Aldrich. Percoll was also purchased from Sigma-Aldrich. iST 96x sample kit (In-StageTip Sample Preparation) was purchased from PreOmics. Evotip PureTM and Evosep One were obtained from Evosep Biosystems, Odense, Denmark. The nanoBoosterCaptiveSpray™ was purchased from Bruker Daltonics. The MMI-L Low Concentration Tuning Mix was obtained from Agilent Technologies, Santa Clara, CA, USA. The Rapid GolgiStain Kit was purchased from FD NeuroTechnologies, Inc., Columbia, MD, United States.

2.2. Animals

Male and female C57BL6/J mice (10–16 weeks old at the beginning of the experiments, Charles River Laboratories Italia, Italy) were group-housed 3–5 per cage under controlled conditions (12-h light/dark cycle, 22 ± 2 ∘C, food, and water ad libitum) and weighed once a week until the end of each experimental protocol. The experimenter handled animals on alternate days during the week preceding the stress procedure. Animals were acclimatized to the testing room at least 1 hour before the beginning of the tests. All experiments were carried out according to EU Directive 2010/63/EU, the Institutional Animal Care and Use Committees of Catania and the Italian Ministry of Health (authorization n° 497/2022-PR).

The experiments complied with the WMA Statement on animal use in biomedical research and/or the EU recommendations (Directive 2010/63/EU) for experimental design and analysis in pharmacology care. Moreover, all animal experiments comply with ARRIVE (Animal Research: Reporting of In Vivo Experiments) guidelines.

2.3. Acoustic startle reactivity (ASR) sessions

Mice were firstly placed in the cylinders of the chambers for a 5-min acclimation period with a 65 dB(A) background noise. Mice were then exposed to 10 acoustic startle stimuli [40 ms — 100 dB(A) noise bursts], which were delivered with variable inter trial intervals of 21, 7, 20, 9, 14, 21, 11, 8, and 23 s to avoid habituation and compensatory mechanisms [24]. Both the magnitude (V max, peak of the response) and latency (T max, time at which the V max occurs) were considered for measurement of the ASR.

2.4. Arousal-based individual screening (AIS) model

The AIS model was applied as described in our previous works [13,15,16]. The day before the traumatic procedure (24-h-restraint stress [14], day 0), a pre-trauma ASR session (day −1) was carried out to assess ASR baseline. This was done to assemble two groups of mice (control and trauma-exposed mice) with similar average of ASR baseline. Control and trauma-exposed mice were given two other ASR sessions, 14 (ASR 1, day 15) and 28 days (ASR 2, day 29) post-trauma respectively. The post-trauma ASR change was analyzed both in terms of magnitude and latency and expressed as percentage of ASR baseline because of the high variability among mice. The post-trauma change of startle magnitude was calculated by using the following formula: [(post-trauma magnitude – baseline magnitude) x 100/baseline magnitude]. The change of startle latency was calculated through the following formula: [(post-trauma

latency – baseline latency) x 100/baseline latency].

To detect traumatic stress susceptibility and resilience, we used an individual screening based on the z-normalization. This tool is extensively used in clinical studies and also successfully employed in rodent studies to measure emotionality dimensions such as ASR, which can diverge across time [25]. The z-scores originating from z-normalization reveal how many standard deviations an observation (X) is above or below the mean [(μ), with its standard deviation (σ)] of a control group: $Z = (X-\mu)/\sigma$. In the AIS model, the long-term changes of ASR are z-normalized to obtain an individual score defined "arousal score".

AROUSAL score = [(X-μ/σ startle magnitude, day 15, 29 + X-μ/σ startle latency, day 15, 29) / 4]. Because most of control mice showed an arousal score below 1, we segregate trauma-exposed mice in susceptible and resilient using a susceptibility threshold of 1. Trauma-exposed mice that exhibited an arousal score ≥ 1 were classified as susceptible, while trauma-exposed mice with an arousal score < 1 were classified as resilient.

2.5. 24-h-restraint stress

A correct air flowing was allowed by drilling 2 holes (0.5 mm of diameter) along the sidewalls and cutting the end of conical tubes 50 ml. A paper towel was placed in each tube to fill the space between the mouse and the cap, and one hole was also drilled in each cup to keep the tails of the mice out of the tube. About 10 tubes containing mice, randomly chosen, were placed in conventional cages (Tecniplast, 425 ×266 x 185 mm) with a level of illumination of 400 lux. During the restraint, mice had no access to food and water. At the end of the restraint, mice were immediately put back to their home cages, with free access to food and water. During the 24 hours of restraint, control mice remained in their home cages in a different room. Trauma-exposed mice were monitored for the recovery of the pre-trauma body weights as well as for the general physical state. Trauma-exposed mice remained group-housed until the end of experiments because we observed no aggressive behavior post-trauma.

2.6. Odor-cued fear conditioning test

We used the odor-cued fear conditioning test developed in our previous work [13] to assess fear reactivity to and avoidance of a trauma-related cue in susceptible and resilient female mice, which were exposed to a neutral odor [lemon oil, the conditioned stimulus (CS)] during exposure to the trauma [the unconditioned stimulus (US)]. Mice were tested in an evenly illuminated (60 ± 1 lux) square open (40 × 40 × 40 cm, Ugo Basile, Gemonio, Italy) after the identification of susceptible and resilient subpopulations (day 29). The behavioral procedure consisted of a no cue exposure session(day 32), and four cue re-exposure sessions, which were performed at different time points (days 33, 40, 54, 75). During the no cue exposure session, mice were individually taken from the home cage and habituated to the open field in the absence of the trauma-related cue for 10 min. During each re-exposure session (10 min), mice were placed in the open field containing the trauma-related cue, a cap for 50 ml falcon tube containing a piece of cotton wool soaked with 600 μl of lemon pure essential oil (Citrus limonum), which was fixed centrally 10 cm from one sidewall. Fear reactivity to the trauma-related cue was detected through the measurement of freezing behavior (% time), which was defined as the complete lack of movement except for that necessary for breathing. Avoidance of the trauma-related cue was identified by assessing explorative behavior of the trauma-related cue, which was defined as the mouse directing its nose toward the cap at a distance of < 2 cm.

The general avoidance-like behavior of control, susceptible and female mice was measured during the first 5 min of the no cue exposure session as previously described [13]. Sixteen square plus one central square (the center) were drawn on the floor of the apparatus. Avoidance-like behavior was quantified by counting the number of entries and the time spent in the center. To circumvent any weighted effect of locomotion on avoidance-like behavior, the number of entries in the center was expressed as center entries ratio that was calculated by the following formula: (center crossings / total crossings) x 100. Behavior of mice was recorded and subsequently analyzed by two experts, well-trained researchers. All behavioral experiments were performed during the light phase from 9:00 a.m.–3:00 p.m.

2.7. Estrous cycle assessment

The estrous cycle assessment was conducted following established protocols, as detailed in previous works [26,27]. After behavioral experiments, female mice were handled gently, positioned on the cage grid, and lifted by the base of the tail. Vaginal lavage was performed using a 1 % PBS solution, delivering approximately 10 μL. The collected vaginal fluid was placed on a glass slide. After air-drying, the samples were stained with Toluidine Blue. Identification of estrous phases was performed using a light microscope.

2.8. Electrophysiological recordings

Extracellular electrophysiological field recordings were performed on 400 μm transverse hippocampal slices (CA3-CA1 synapses) of susceptible and resilient mice of both sexes, as previously reported [28]. Experiments were conducted by an operator who was blind to the subpopulation of mice. Three days after the segregation in subpopulations, mice were randomly selected and euthanized via cervical dislocation before brain removal. Slices were placed in a recording chamber and perfused (1–2 ml/min) with artificial cerebrospinal fluid (ACSF) solution containing (in mM): 124 NaCl, 4.4 KCl, 1 Na_2HPO_4, 25 $NaHCO_3$, 2 $CaCl_2$, 2 $MgCl_2$, and 10 glucose, maintained at 29° C and continuously bubbled with 95 % O_2 and 5 % CO_2. After 120 min of recovery, field excitatory post-synaptic potentials (fEPSPs) were recorded in CA1 stratum radiatum using a glass electrode filled with ACSF in response to Schaffer collateral stimulation by a bipolar tungsten electrode. We first measured basal synaptic transmission (BST) by stimulating with a series of increasing voltage pulses ranging from 5 to 35 V. For LTP experiments, a baseline was established by recording every minute for 15 min by stimulating at a voltage able to evoke a response of 35 % of the maximum evoked response in BST. LTP was induced using a theta-burst stimulation protocol, which consisted of trains of 10 × 100 Hz bursts with five pulses per burst and a 200 ms inter-burst interval set at the test pulse intensity. LTP was recorded for 120 after tetanus. All experiments assessing short-term plasticity were conducted in the presence of APV (50 μm), a selective competitive NMDA receptor antagonist. For paired pulse facilitation (PPF) experiments, two paired pulses were administered at varying time intervals: 10, 20, 30, 40, 50, 100, 200, 500, and 1000 ms. PPF was quantified by measuring the synaptic response of the second stimulus as a percentage of the response to the first delivered stimulus. Post-tetanic potentiation (PTP) was evaluated using a stimulation interval of every 5 s over a 2-minute duration, following the procedure outlined for LTP baseline. A theta-burst protocol was used for stimulation, with recordings taken for a subsequent 3 min. Synaptic fatigue was induced using two distinct protocols. In the first, a stimulation frequency of 10 Hz was maintained for 30 s. In the second protocol, a train of 20 pulses at 100 Hz was delivered. To assess recovery after vesicle pool depletion, following the 100 Hz stimulation, additional pulses were delivered with different interpulse intervals: 125 ms from the first to the seventh pulse, 1000 ms between the seventh and eighth pulse, and 3000 ms between the eighth and ninth pulse.

2.9. Preparation of purified hippocampal synaptic terminals (synaptosomes)

Three days after the segregation in subpopulations, purified hippocampal synaptic terminals (synaptosomes) were isolated by using

discontinuous Percoll gradient centrifugation as previously described [29]. Hippocampi were isolated after microdissection and placed into 1.5 ml of ice-cold SET. Tissues were homogenized on ice using 20 up and down strokes. The resulting homogenate was transferred into a 2 ml Eppendorf tube and centrifuged at 1,000 g at 4° C for 10 min. The supernatant was carefully transferred into a polycarbonate tube and placed on ice. The remaining pellet was resuspended in 1.5 ml ice-cold SET and again centrifuged at 1000 g at 4° C for 10 min. The second supernatant was collected and combined with the previous one, obtaining a final volume of 3 ml. The pooled supernatant was subjected to a first step of ultracentrifugation at 21000 g at 4° C for 10 min using the T-8100 fixed angle rotor with the Thermo Scientific Sorwall WX100 ultracentrifuge. During this period the lower two layers of Percoll gradient were prepared in polycarbonate tubes, using 10 % Percoll and 24 % Percoll. First, 1 ml of 10 % Percoll was added to the tube, then 1 ml 24 % Percoll was slowly introduced to the bottom of the tube creating a discontinuous gradient. At the end of the ultracentrifugation, the resulting pellet was resuspended in 1 ml of 3 % Percoll and slowly layered above the 10 % Percoll. Then, the tube was subjected to a second step of ultracentrifugation at 30,800 g at 4° C for 9 min using slow acceleration (~1 min from 0 to 500 rpm followed by normal acceleration) and no deceleration (no brakes). This step lasted ~45 min. The material on the top of the gradient was removed; the material between the layers 24 % and 10 % Percoll, enriched in synaptosomes, was collected (~0.5–0.6 ml) into a 2 ml Eppendorf tube and diluted with 1 ml ionic medium. The recovered fraction was centrifuged at 20,000 g at 4° C for 15 min. The pellet was recovered and transferred into a new 1.5 ml Eppendorf tube and again centrifuged at 20,000 g at 4° C for 10 min.

2.10. Synaptoproteomic profiling

Proteomic profiling was performed in hippocampal synaptosomes (3 pools of 4 animals for each experimental condition). To ensure robustness and account for experimental variability, three technical replicates for each pool were produced.

2.10.1. DIA-PASEF label free analysis: sample preparation

Cell extracts were prepared using the iST 96x sample kit (In-StageTip Sample Preparation) according to the manufacturer instructions using adapters for tube reaction. Briefly, 50 µl of lysis buffer solution were added to 100 µg of protein extracts and heated to 95 °C for 10 min shaking (1000 rpm) followed by ten cycles of 30 s of sonication. Proteins were transferred into a cartridge and after the addition of the digestion solution were digested for 3 h at 37 °C. Digestion was stopped by adding the "STOP" solution, and peptide purification was achieved by centrifugation for 2 min at 3800 g, followed by two rounds of washing and two rounds of elution into the collection tubes using the provided solutions. Peptides were dried in a vacuum centrifuge, resuspended in "LC-LOAD" solution in a concentration of 1ug/ul for MS analysis and shaken for 5 min (500 rpm).

2.10.2. Mass spectrometry analysis

Peptides were loaded into a disposable trap column, Evotip PureTM following the manufacture protocol. An amount of 400 ng of peptides for each sample was injected in triplicate into Evosep One LC system coupled online with timsTOF fleXTM (Bruker Daltonics, Bremen, Germany) mass spectrometer, as already reported (with some modifications) [30]. Desalted and concentrated peptides were separated into an analytical 8 cm column (PepSep C18, 8 cm Performance column, particle size of 1.5 µm and internal diameter of 150 µm) at a temperature of 40° C. A gradient of solvent A (0.1 % FA) and solvent B (ACN (LC-MS grade - LiChrosolv®) + 0.1 % FA) was used for the separation using a 21 min (60 SPD) method. The eluted peptides were ionized using a nanoBoosterCaptiveSpray™. The mass spectrometer was operated in DIA (Data Independent Acquisition)-PASEF (Parallel Accumulation-Serial Fragmentation) mode. Ions were scanned in positive mode, over an m/z of 100–1700 and a mobility range of 0.85–1.30 V·s/cm^2. Dry gas flow was 3.0 l/min at 180°C and capillary voltage was 1400 V. For tandem mass PASEF analysis, the cluster of mono-charged ions was excluded to reduce the complexity of MS2 spectra using the following parameters: m/z 475–1000 Da and 0.85–1.27 V·s/cm^2, the estimated cycle time for each PASEF analysis was 0.95 s with a total of 8 cycles using DIA windows of 25 Da.

The mass spectrometer was calibrated for mass and ion mobility accuracy, using a mix of ten standards with a known mass (MMI-L Low Concentration Tuning Mix). For calibration on nano-source, three specific lock masses (622.0290 m/z, 922.0098 m/z and 1221.9906 m/z) have been applied on a filter.

2.10.3. Data processing

Raw data were elaborated by using SpectronautTM (v.17, https://biognosys.com) following a library-free processing method based on the Mus musculus (Swissprot database, downloaded on 12–05–2023, 17155 entries). The parameters were set as follows: Trypsin and LysC as enzymes, carbamidomethyl (C) as fixed modification, acetylation (protein N-term), and oxidation (M) as variable modifications, 1 % FDR at precursor and protein levels. Abundance values were automatically cross-run normalized. Proteins were considered identified only if they had at least one unique peptide. Data were finally exported into Excel for further analysis.

2.10.4. Differential expression analysis

Differential protein expression analysis was performed with the DeqMS (v. 1.12.1) package [31] in R (v. 4.1.2). DEqMS builds on top of Limma [32], and improves it with proteomics data specific properties, accounting for variance dependence on the number of quantified peptides or PSMs for statistical testing of differential protein expression. Analysis was performed on the average of the expression levels obtained from the three technical replicates. Data were log-transformed and centered on the median before applying DEqMS. The relationship between protein expression and the stress condition was modelled in the form of protein expression = β_1 C_M+ β_2 C_F + β_3 R_M + β_4 R_F + β_5 S_M + β_6 S_F and analyzed with "lmFit" integrated in DeqMS package. The following 11 contrasts were tested: 1) TE male mice (susceptible + resilient) vs C male mice; 2) TE female mice (susceptible + resilient) vs C female mice; 3) resilient male mice vs control male mice; 4) resilient female mice vs control female mice; 5) susceptible male mice vs control male mice; 6) susceptible female mice vs control female mice; 7) susceptible male mice vs resilient male mice; 8) susceptible female mice vs resilient female mice. 9) susceptible female mice vs susceptible male; 10) resilient female mice vs resilient male; 11) control female vs control males. The function `spectraCounteBayes` in DEqMS was used to correct bias of variance estimate based on minimum number of peptides per protein used for quantification.

Only proteins that were expressed across all the samples were considered. In total, we identified 5063 proteins that met this criterion and were included in our further investigations. Differentially expressed proteins (DEPs) were considered for an adjusted p value < 0.05. Principal Component Analysis (PCA) was performed with prcomp tool in stats R package.

2.10.5. Pathways enrichment analysis

Enrichment analysis was performed using WebGestaltR v. 4.0.3 [33] and the Gene Set Enrichment Analysis (GSEA) method. The categories considered for the analysis were those of the Mouse MSigDB Collection M2 Reactome canonical pathways (m2.cp.reactome.v2023.1.Mm.entrez.gmt). Only enrichment categories with more than 10 genes and less than 500 genes were analyzed, and categories with FDR < 0.10 were reported. In total, we annotated 4713 unique Entrez Gene IDs, of which 2877 were assigned to functional categories used in the enrichment analysis.

2.11. Dendritic morphology

For dendritic morphology analysis, control, susceptible and resilient mice of both sexes were euthanized via cervical dislocation three days after identification. Golgi-Cox staining was carried out using the Rapid GolgiStain Kit as previously described [34,35]. Hemispheres were coronally sliced (250 μm) using a cryostat (Leica CM 1520, Leica Biosystems, Buccinasco, Italy). CA1 and dentate gyrus (DG) areas of hippocampus were identified under visible light on an inverted microscope (Cell Observer, equipped with the Zen 3.5 Blue edition software, Zeiss, Milano, Italy). Z-stacks (1 μm per Z-step size) of 5–8 CA1 or DG pyramidal neurons per animal with untruncated branches were acquired using a × 63 oil objective. Collapsed Z-stacks were analyzed using the Fiji ImageJ software [36] and dendrites were reconstructed using the FilamentTracer function [37]. Dendritic length was assessed using the SNT option of the "neuroanatomy" plug-in [38]. Dendritic spines (55–65 μm secondary dendrites) were counted using the plug in "dendritic spine counter" (v 1.6.3) and expressed as density: n spines/μm. CA1 basal and apical dendrites were considered separately. Analyses were performed on 6/8 mice per group (5–8 neurons per mouse).

2.12. Statistical analysis

Sample size was determined by using power analysis and was thus similar to that of studies using related methods. Each experimental group consisted of a minimum of five mice. Data were analyzed using GraphPad Prism 8 (GraphPad Software, La Jolla, CA, USA). To assess data distribution, the D'Agostino-Pearson omnibus normality test was carried out. The Levene's test was also used to verify equality of variances. All data assumed a normal distribution and then they were subjected to parametric tests (one, two-way ANOVA, two-way ANOVA with repeated measures when appropriate and three-way ANOVA; see figure legends for details). A chi-squared test was performed to assess the percentage of susceptibility/resilience according to the sex. For all data analyses, upon confirmation of significant main effects, differences among individual means were assessed using Bonferroni post-hoc test. P values of < 0.05 were considered significant. The estimate of dispersion is shown as the standard error of the mean (s.e.m.), and variances were found to be similar among groups. All data are presented as means ± s.e.m.

3. Results

3.1. Female mice exposed to 24h-restraint-stress were more susceptible to develop PTSD-related phenotypes than male mice

To assess the effectiveness of the AIS model in mimicking sex-biased traumatic stress susceptibility, we firstly tested both males (n = 36 trauma-exposed mice) and females (n = 38 trauma-exposed mice) using the experimental procedure established for this model (Fig. 1A). The AIS model is effective in identifying susceptible and resilient female mice long after exposure to the trauma. The calculation of the arousal score allowed us to segregate trauma-exposed mice of both sexes in susceptible and resilient mice (Fig. 1B). During the ASR1, male susceptible

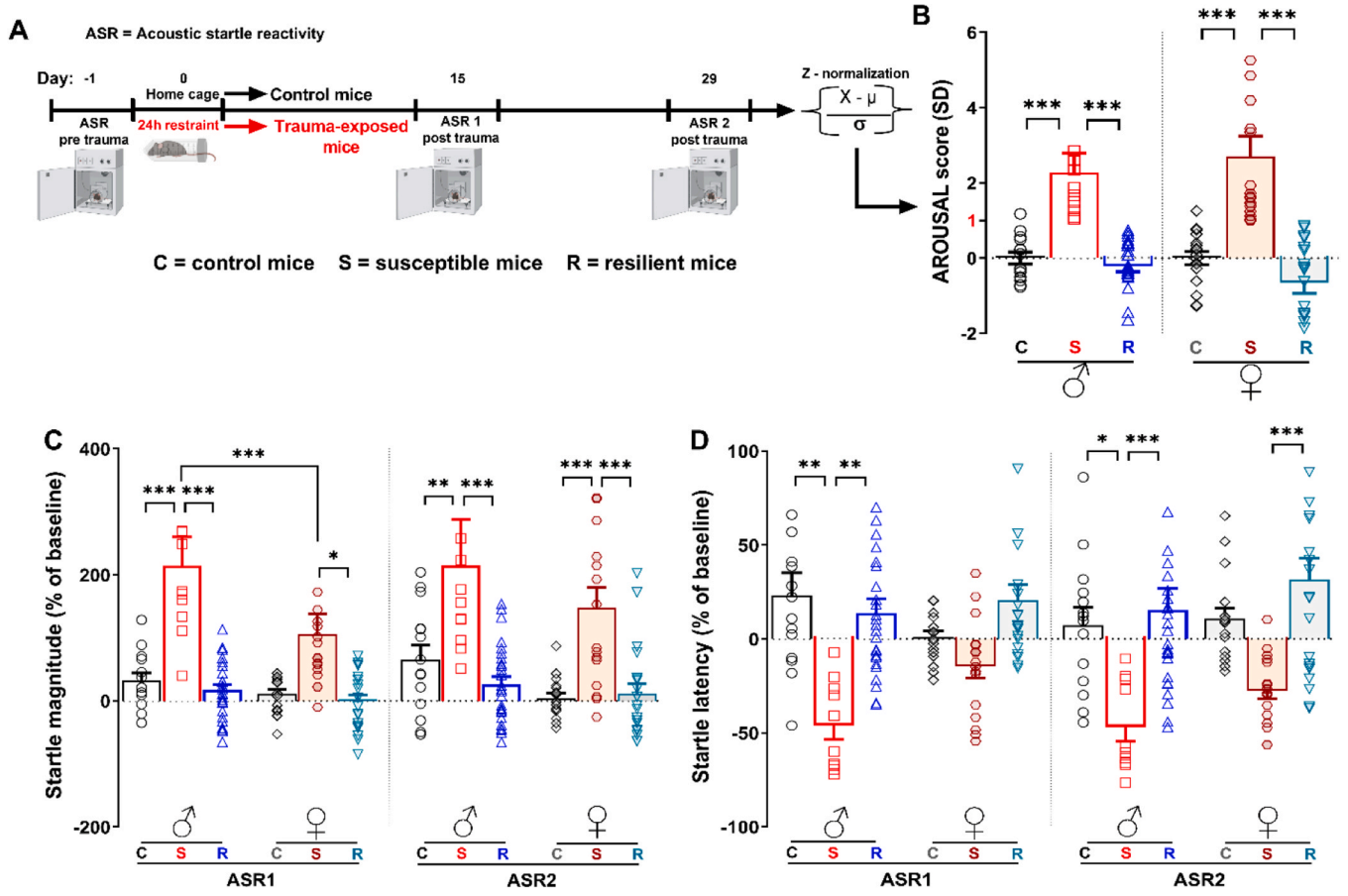

Fig. 1. *The AIS model was effective in identifying susceptible and resilient mice of both sexes.* (A) Experimental procedure of the AIS model. (B) Arousal score of control male mice (n = 14), susceptible male mice (n = 10), resilient male mice (n = 26), control female mice (n = 16), susceptible female mice (n = 17), resilient female mice (n = 21), (*Stress susceptibility*, $F_{(2, 99)} = 44.61$; $P < 0.0001$). (C) Startle magnitude (% of baseline, *Stress susceptibility*, $F_{(2, 99)} = 33.72$, $P < 0.0001$; *Sex*, $F_{(1, 99)} = 8.740$, $P = 0.0039$. (D) Startle latency (% of baseline, *Stress susceptibility*, $F_{(2, 99)} = 30.17$, $P < 0.0001$). Two-way repeated measures (RM) ANOVA or three-way ANOVA followed by Bonferroni post hoc test: *$P < 0.05$, **$P < 0.01$ and ***$P < 0.001$. Values are expressed as means ± s.e.m.

mice exhibited a significant higher startle magnitude compared to respective control and resilient mice, while female susceptible mice exhibited a significant higher startle magnitude compared to respective resilient mice (Fig. 1C). Noteworthy, during the ASR 1 male susceptible mice exhibited a significant higher startle magnitude compared to female susceptible mice, suggesting that susceptible males have a stronger startle reactivity than females soon after stress exposure (Fig. 1C). This sex difference was not found during the ASR 2, in which either male or female susceptible mice showed a significant higher startle magnitude compared to respective control and resilient mice (Fig. 1C). Regarding the measurement of startle latency, male susceptible mice exhibited a significant decrease of startle latency in comparison with respective control and resilient mice during both ASR sessions (Fig. 1D). By contrast, female susceptible mice exhibited a significant decrease of startle latency in comparison with respective resilient mice during the ASR 2 (Fig. 1D). Estrous cycle did not affect the startle reactivity of both susceptible and resilient female mice, during the ASR sessions (Fig. S1A-D).

In this first experiment (experiment 1) performed to assess the effectiveness of the AIS model as well as to perform electrophysiological recordings, we identified: 10 male susceptible mice (27.8 %), 26 male resilient mice (72.2 %), 17 female susceptible mice (44.7 %) and 21 female resilient mice. In the second experiment (experiment 2; n = 31 male and n = 25 female trauma-exposed mice) performed to evaluate hippocampal structural plasticity, we identified: 7 male susceptible mice (22.6 %), 24 male resilient mice (75 %), 9 female susceptible mice (36 %) and 16 female resilient mice (64 %). In the third experiment (experiment 3; n = 40 male and n = 39 female trauma-exposed mice) carried out to assess the hippocampal synaptoproteomic landscape, we identified: 10 male susceptible mice (25 %), 30 male resilient mice (75 %), 14 female susceptible mice (35.9 %) and 25 female resilient mice (64.1 %). In the last experiment (experiment 4; n = 46 male and n = 45 female trauma-exposed mice), which we performed to evaluate the effects of the Rac1/Rac3 GTPases inhibitor EHop-016 on the impairment of LTP, we identified: 13 male susceptible mice (28,3 %), 33 male resilient mice (71,7 %), 14 female susceptible mice (31.1 %) and 31 female resilient mice (68.9 %). We thus analyzed the percentage of trauma susceptibility/resilience considering all susceptible and resilient mice of both sexes identified through these experiments. Importantly, a Chi-square test revealed a significant more susceptibility of female mice to the trauma compared to male mice (Fig. 2A).

Some control, susceptible and resilient mice identified in the first experiment were also tested two months post-trauma (day 56) in a third ASR session (ASR 3). Susceptible female mice developed a long-lasting hyperarousal, given that they still exhibited a significant higher startle magnitude (Fig. 2B) as well as a significant lower startle latency (Fig. 2C), in comparison with both control and resilient female mice, during a third ASR session performed two months post-trauma.

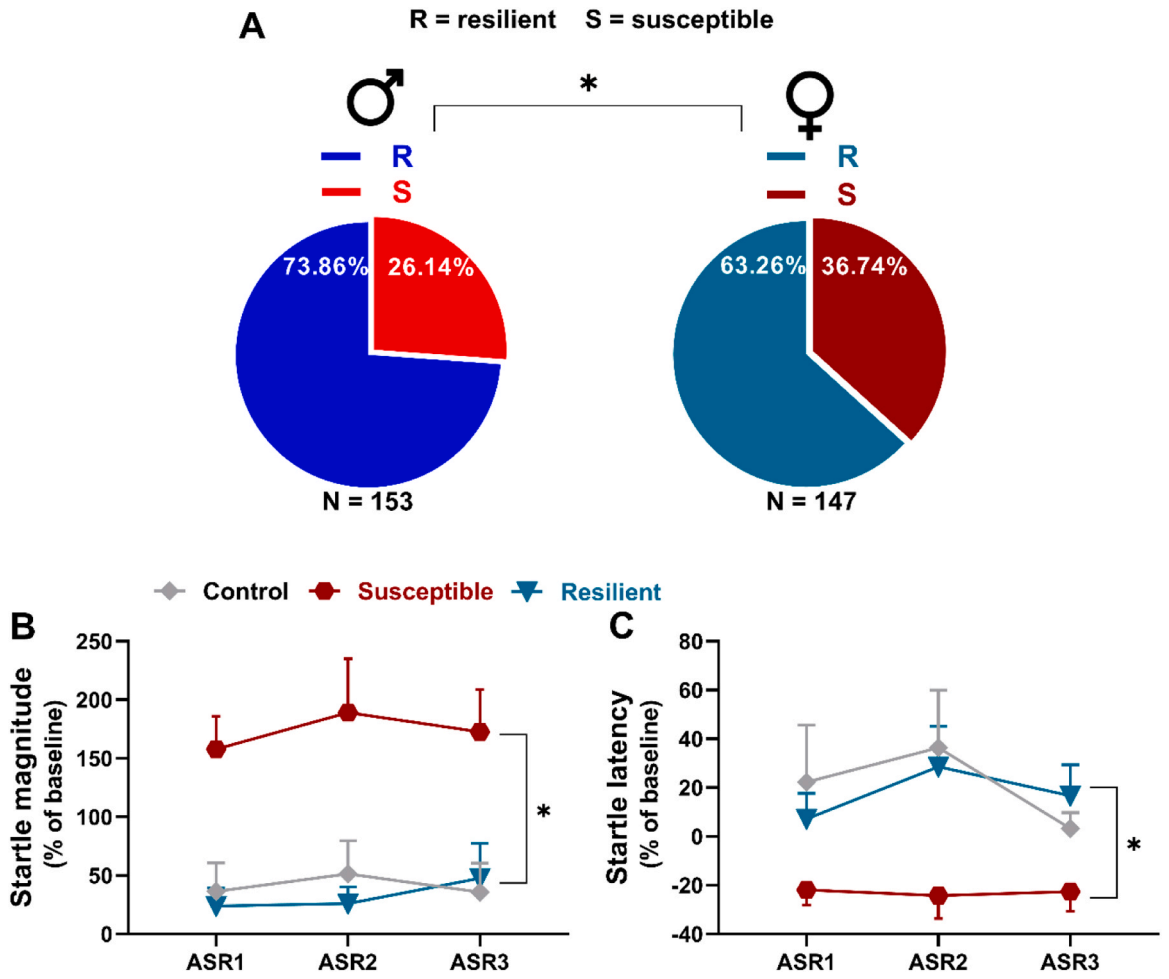

Fig. 2. *Trauma-exposed female mice were more susceptible to develop persistent PTSD-related phenotypes than trauma-exposed male mice.* (A) Percentage of susceptible and resilient mice of both sexes [X^2 (1, N = 300) = 3.908, p = 0.0408]. (B) Startle magnitude (% of baseline) (*Stress susceptibility,* $F_{(2, 19)} = 14.33$, P = 0.0002) (C) Startle latency (% of baseline) (*Stress susceptibility,* $F_{(2, 19)} = 4.375$, P = 0.0274;) of some control female mice (n = 5), susceptible female mice (n = 6) and resilient female mice (n = 11) identified through the AIS model and further tested two months post-trauma (ASR 3). Chi-square test and two-way RM ANOVA followed by Bonferroni *post hoc* test: *P < 0.05. Values are expressed as means ± s.e.m.

In our previous study, we demonstrated that susceptible male mice exhibited significantly increased of avoidance-like behavior and fear reactivity to a trauma-related cue [13]. Here we found that also susceptible female mice showed increased avoidance-like behavior and long-lasting exaggerated fear responses to a trauma-related cue. During the no cue exposure session (day 32) of the odor-cued fear conditioning test (Fig. S2A), there were no significant differences in center entries ratio among control, susceptible and resilient female mice (Fig. S2B). However, susceptible female mice but not female resilient mice exhibited a significant decrease in time spent in the center of the open field compared to control mice (Fig. S2C). Total crossings remained comparable across groups (Fig. S2D), indicating that the avoidance-like behavior observed was not attributable to differences in general locomotor activity.

During the no cue exposure session (day 32), basal freezing in the absence of cue was comparable among groups (Fig. S2E). During the first re-exposure session (day 33), susceptible and resilient female mice exhibited significantly elevated cue avoidance compared to control mice, as indicated by reduced exploration time of the trauma-related cue (Fig. S2F). Importantly, susceptible female mice showed a progressive and sustained freezing response across multiple cue re-exposure sessions (days 33, 40, 54, 75), with freezing levels significantly higher than control and resilient mice at all timepoints (Fig. S2G). In contrast, resilient female mice showed freezing levels similar to control female mice, indicative of normal fear memory recall without exaggerated fear responses.

3.2. Hippocampal long-term potentiation impairment is associated with traumatic stress susceptibility regardless of sex

We next conducted electrophysiological studies at CA3-CA1 hippocampal synapses (Fig. 3A) to test the hypothesis that traumatic stress could induce sex-dependent alterations of synaptic transmission and plasticity. LTP, a form of synaptic plasticity underlying memory formation [39], was significantly impaired in susceptible male and female mice (Fig. 3B-D), whereas it remained unaffected in resilient mice of both sexes (Fig. 3B-D). These findings confirm our previous observations showing LTP impairment in susceptible male mice [13]. Analyses of BST in slices from control, susceptible and resilient mice of both sexes revealed no differences among groups (Fig. 3E, F).

To further investigate the effects of traumatic stress on synaptic function, we examined different forms of presynaptic short-term plasticity. Analysis of PPF, which depends on presynaptic mechanisms regulating neurotransmitter release, showed no differences in slices from resilient or susceptible mice of both sexes (Fig. 3G, H). However, a significant difference was observed between control female and male mice, indicating subtle sex-dependent variations in presynaptic function under baseline conditions. Neurotransmitter release was also assessed by evaluating PTP, an index of neurotransmission efficiency, and no significant differences were found related to the sex or trauma phenotype (Fig. 3I, J). We next assessed synaptic fatigue, which reflects the ability of the synapse to recover from neurotransmitter depletion. To comprehensively evaluate this phenomenon, we employed different stimulation protocols. Under the 10 Hz protocol, control female mice showed faster vesicle depletion compared to control males. However, exposure to traumatic stress did not affect synaptic fatigue in either susceptible or resilient mice (Fig. 3K, M). No differences were observed in slices from both male or female resilient and susceptible mice subjected to the 100 Hz protocol, in terms of either vesicular depletion or recovery of neurotransmitter release (Fig. 3L, N).

Collectively, our findings indicate that susceptible mice, regardless of sex, exhibit a pronounced impairment in LTP, whereas BST and short-term synaptic plasticity remain unaltered.

3.3. Traumatic stress triggered sex- and phenotype-dependent dendritic remodeling of hippocampal neurons

Because we found deficits of long-term synaptic plasticity in the hippocampus of susceptible mice of both sexes, we wondered whether this was associated with changes at the level of dendritic remodeling of hippocampal neurons. In this regard, previous studies have demonstrated that LTP is consistently accompanied by structural modifications of dendritic spines, including spine enlargement and morphological remodeling in hippocampal neurons [40]. Thus, we evaluated total length and spine density of the basal and apical dendritic arbor of CA1 pyramidal neurons and DG granule neurons.

The length of CA1 apical dendrites was significantly increased only in susceptible male mice compared to both control and resilient male mice, while no changes were observed in female mice of both phenotypes (Fig. 4A). Conversely, length of CA1 basal dendrites was significantly decreased in control and resilient female mice compared to control and resilient male mice (Fig. 4B). Regarding DG granule neurons, dendritic length was significantly reduced exclusively in resilient female mice compared to both control female and resilient male mice (Fig. 4C).

Spine density analysis of CA1 apical dendrites uncovered no significant differences among groups (Fig. 5A). In contrast, CA1 basal dendritic spine density was significantly increased exclusively in susceptible male mice in comparison with both control and resilient male mice (Fig. 5B). Finally, spine density of DG granule neurons was significantly higher in control females compared to control male mice (Fig. 5C).

3.4. Traumatic stress induced sex- and phenotype-dependent changes in the synaptoproteomic landscape of the hippocampus

To assess whether the synaptic and structural plasticity alterations were accompanied by molecular changes at synapses, we then performed a synaptoproteomic analysis of the hippocampus. Synaptosomes derive from synaptic boutons and express proteins involved in mechanisms subserving synaptic plasticity, thus allowing the evaluation of synaptic-specific changes in protein expression [41].

Principal component analysis (PCA) was performed to identify outlier samples. All samples were considered suitable for further analysis as no outliers were detected. No separate clusters were observed for control or trauma-exposed mice (Figure S3A) either for males or females (Fig. S3B). None of the 5063 tested proteins individually exhibited a significantly altered expression profile (FDR < 0.05) in any comparison. Nevertheless, we adopted a GSEA approach, a threshold-free method that analyzes all genes based on their differential expression rank, to evaluate whether the proteins exhibiting the most pronounced up or down-regulation were enriched in specific biological pathways with small yet coordinated trends. The GSEA analysis highlighted sex- and phenotype-dependent alterations at synaptoproteome level (Fig. 6, Fig. S4, Tables S1–10). Considering the comparison between trauma-exposed (both susceptible and resilient) and control male mice, we observed a reduction of protein-sets related to synaptic transmission and an enrichment of proteins implicated in the cellular localization and stability of steroid hormone receptors (Fig. S4; Table S1). The limited number of significant pathways found enriched is likely attributable to the heterogeneity within the group of trauma-exposed mice. Indeed, after stratifying trauma-exposed male mice in susceptible and resilient subpopulations, it became evident that the two groups have different proteomic profiles (Fig. 6). When resilient male mice were compared with control male mice, we found a downregulation of pathways related with the proteasome activity and an upregulation of proteins belonging to the pathway of neurexins and neuroligins, synaptic cell-adhesion molecules mediating trans-synaptic signaling and shaping neural network properties [42]. We also noticed an enrichment of proteins associated with pathways linked to glycosaminoglycans (GAG) among upregulated proteins (Fig. 6; Table S2). Differently, when susceptible

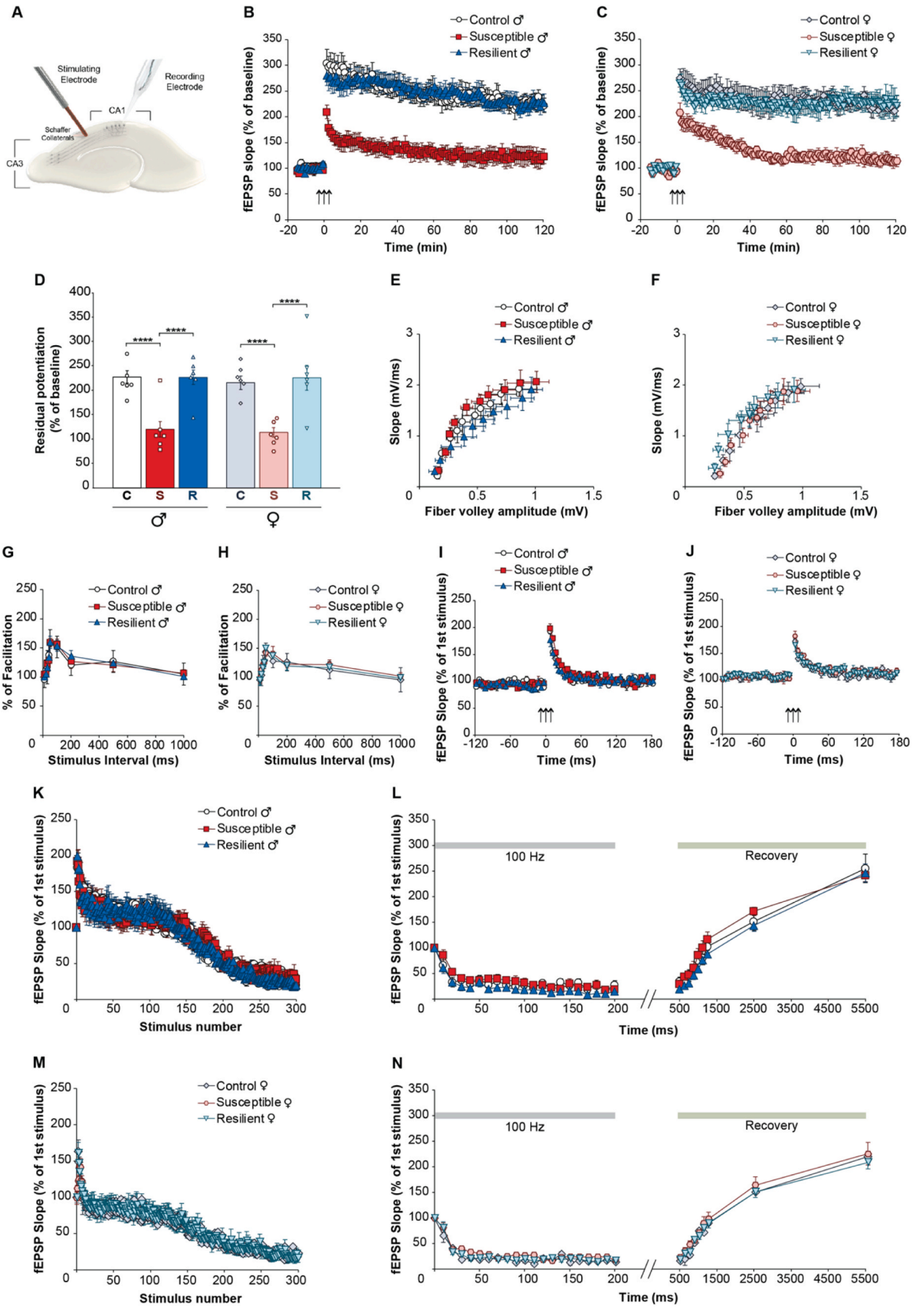

(caption on next page)

Fig. 3. *Long-term synaptic plasticity was impaired in susceptible mice of both sexes, while short-term synaptic plasticity remained unaffected.* (A) Representative image of electrodes placement within the hippocampal slice. (B, C) LTP remained unaltered in resilient male (B) and female (C) mice compared to controls (males: $F_{(1,12)} < 0.0001$, $P = 0.983$ n = 7/7 slices from 4/4 animals; females: $F_{(1,12)} = 0.117$, $P = 0.738$ n = 7/7 slices from 4/4 animals). In contrast, LTP was notably impaired in both susceptible male and female mice compared to controls (males: $F_{(1, 13)} = 28.168$, $P < 0.0001$, n = 8 slices from 5 animals females: $F_{(1, 12)} = 30.043$, $P < 0.0001$, n = 7 slices from 4 animals). No differences were detected among male and female resilient ($F_{(1,12)} = 1.387$, $P = 0.262$), susceptible ($F_{(1,13)} = 0.003$, $P = 0.961$) or controls mice ($F_{(1,12)} = 0.398$, $P = 0.540$). (D) Analysis of residual potentiation (averaged over the last 5 min of LTP recording, 120 min post-tetanus) confirmed the LTP impairment in susceptible mice and showed no sex-related differences ($F_{(5, 37)} = 11.776$, $P < 0.0001$ among all groups; Bonferroni post-hoc: controls vs susceptible males $P < 0.0001$; controls vs susceptible females $P = 0.001$). (E, F) Analysis of Basal Synaptic Transmission (BST) revealed no significant differences in fEPSP slope or fiber volley (FV) among control, susceptible and resilient mice (males and females n = 9 slices from 5 animals for all conditions). (G, H) PPF was not affected by traumatic stress exposure both in males (control n = 12 slices from 7 animals; susceptible n = 12/4; resilient n = 13/4) and females (control n = 11/4; susceptible n = 12/4; resilient n = 15/4). Sex-related differences were found only in control mice ($F_{(1, 21)} = 5.757$, $P = 0.026$). (I, J) No changes were found in PTP in either males (J) (control n = 12 slices from 4 animals; susceptible n = 14/4; resilient n = 11/4) or females (K) (control n = 12 slices from 4 animals; susceptible n = 10/4; resilient n = 11/4). (L, M) No stress-related changes were observed during synaptic fatigue at 10 Hz in either males (L) (control n = 10 slices from 4 animals; susceptible n = 10/4; resilient n = 10/4) or females (M) (control n = 12 slices from 4 animals; susceptible n = 11/4; resilient n = 13/4). Conversely sex-related differences were found in all conditions (controls: $F_{(1, 20)} = 1.101$, $P < 0.0001$; susceptible: $F_{(1, 19)} = 4.552$, $P = 0.0461$; resilient: $F_{(1, 21)} = 4.451$, $P = 0.0471$). (O, P) No changes were observed during synaptic fatigue at 10 Hz in either males (O) (control n = 11 slices from 4 animals; susceptible n = 11/4; resilient n = 11/4) or females (P) (control n = 11 slices from 4 animals; susceptible n = 12/4; resilient n = 13/4). Two-way for repeat-ed measured ANOVA or One-way ANOVA. Post hoc comparisons were made using the Bonferroni test: ****$P < 0.0001$. All values are presented as means ± s.e.m.

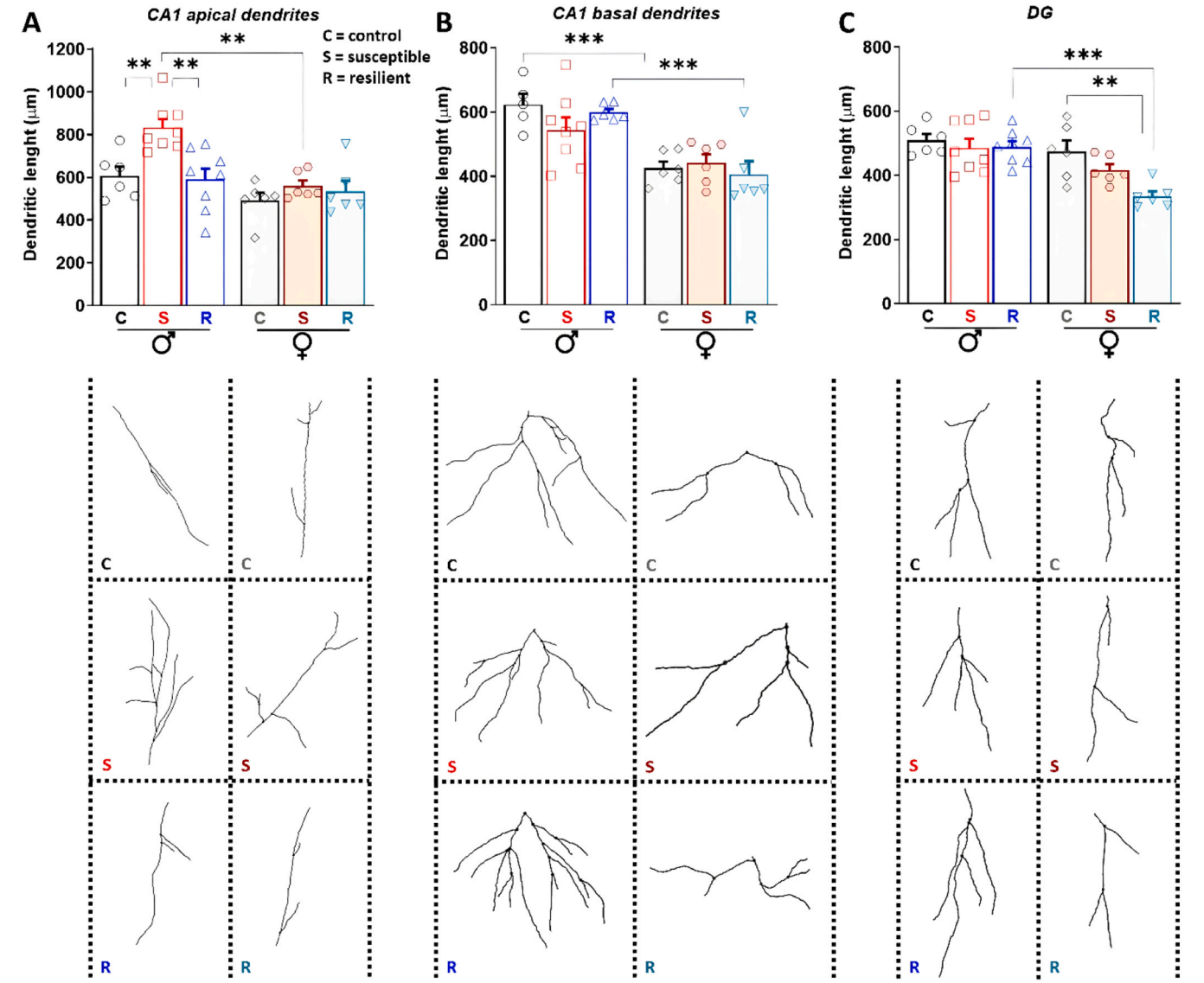

Fig. 4. *Traumatic stress triggered sex- and susceptibility/resilience-dependent changes in dendritic length of hippocampal neurons.* (A) Total length of CA1 apical dendrites of pyramidal neurons (*Sex*, $F_{(1, 34)} = 17.09$, $P = 0.0002$; *Stress susceptibility*, $F_{(2, 34)} = 7.122$, $P = 0.0026$; *Sex x Stress susceptibility* $F_{(2, 34)} = 3.507$, $P = 0.0412$). (B) Total length of CA1 basal dendrites of pyramidal neurons (Sex, F (1, 31) = 38.90, $P < 0.0001$). (C) Total dendritic length of DG granule neurons (*Sex*, $F_{(1, 34)} = 19.54$, $P < 0.0001$; *Stress susceptibility*, $F_{(2, 34)} = 5.583$, $P = 0.0080$; *Sex x Stress susceptibility* $F_{(2, 34)} = 3.318$, $P = 0.0483$). Two-way ANOVA followed by Bonferroni post hoc test: *$P < 0.05$, **$P < 0.01$, ***$P < 0.001$. Data are shown as means ± s.e.m. Insets: representative morphological reconstructions of dendritic trees performed with the Fiji ImageJ Neuroanatomy plugin. C: control mice; S: susceptible mice; R: resilient mice.

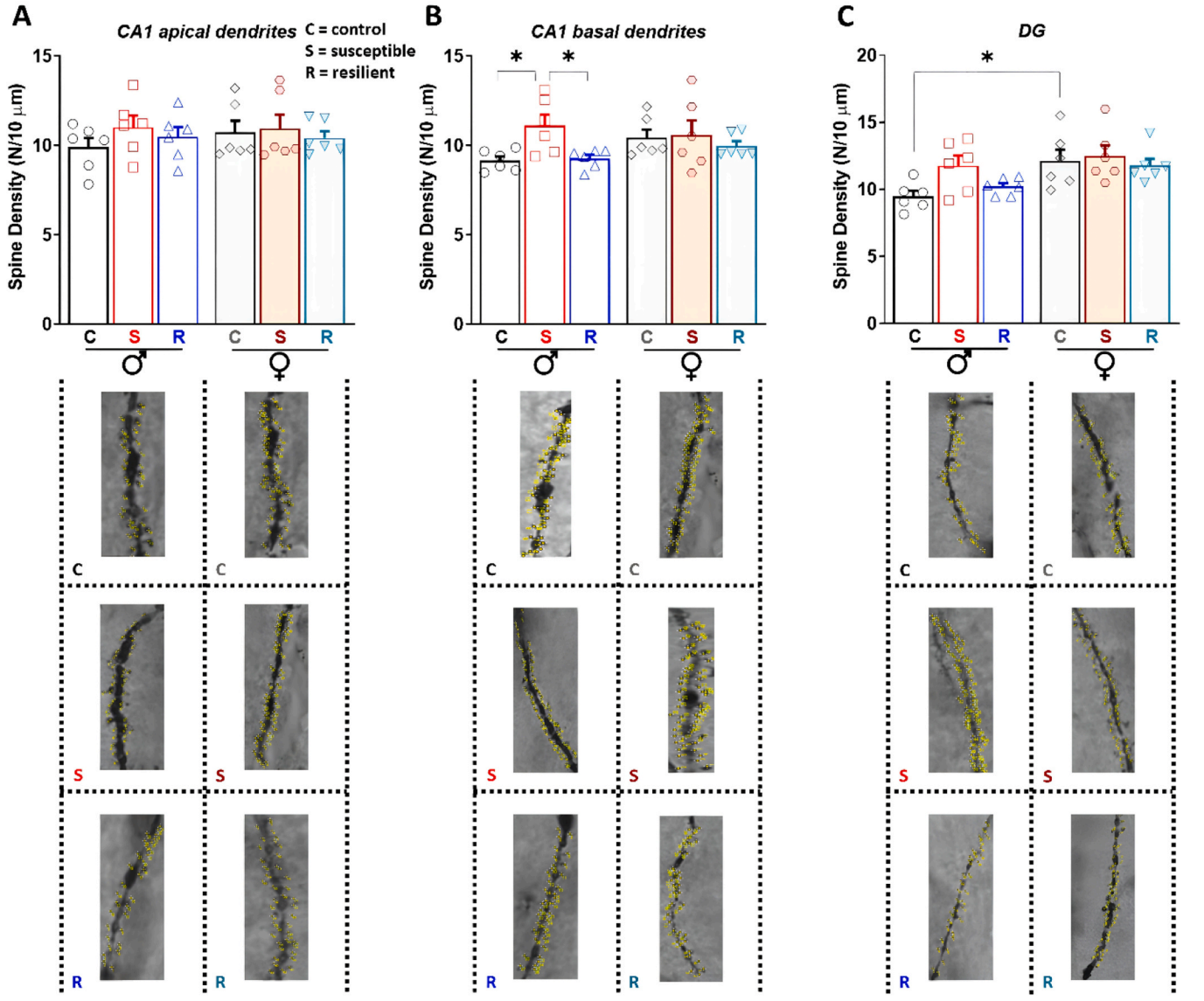

Fig. 5. *Traumatic stress induces sex- and susceptibility/resilience-dependent changes in spine density of hippocampal neurons.* (A) Spine density (number of spines/10 μm) in CA1 apical dendrites of pyramidal neurons. (B) Spine density in CA1 basal dendrites of pyramidal neurons (*Stress susceptibility*, $F_{(2, 30)} = 3.728$, $P = 0.0358$). (C) Spine density in DG granule neurons (*Sex*, $F_{(1, 30)} = 9.924$, $P = 0.0037$). Two-way ANOVA followed by Bonferroni post hoc test: *$P < 0.05$. Values are expressed as means ± s.e.m. Insets: representative images of Golgi-Cox-stained dendrites and automatic identification/counting of spines by using the Fiji ImageJ Dendritic spine counter plugin. C: control mice; S: susceptible mice; R: resilient mice.

male mice were compared with control male mice, a significant number of pathways related to signal transduction were found enriched among the downregulated proteins. Some of these pathways oversee the activation of GABAergic receptors and the cellular response to stimulation, while others play a crucial role in maintaining ionic balance through potassium channels. On the contrary, proteins implicated in the cellular localization, stability of steroid hormone receptors as well as in several pathways related to RHO Family GTPases were upregulated (Fig. 6; Table S3).

The different proteomic profile between resilient and susceptible male mice is also corroborated by the direct comparison between the two groups that revealed 55 significantly enriched protein-sets (FDR < 0.05) among up and down regulated proteins (Fig. 6; Table S4). Proteins downregulated in susceptible male mice are enriched in pathways associated with the functioning and regulation of cells engaged in transmitting neural signals, while proteins downregulated in resilient male mice are enriched in pathways associated with proteasome function.

A different pattern was found by evaluating female mice. Comparing trauma-exposed female mice with control female mice, we detected a prominent presence of protein-sets related to energy metabolism and mitochondrial functions at the top of ranked protein list (Fig. S4; Table S5). Remarkably, the enrichment of these pathways remained evident even when stratifying female mice into susceptible and resilient groups, suggesting no major synaptoproteomic changes between susceptible and resilient female mice (Fig. 6; Tables S6 and S7). Notably, in the resilient group we also observed a downregulation of pathways related to the metabolism of glycosaminoglycans (GAGs) and sphingolipids towards the bottom of our ranked list (down-regulated proteins in resilient females) (Fig. 6; Table S6). No significant differences were observed in the comparison between susceptible and resilient females.

We also directly compared female and male mice (Fig. S4; Tables S8-S10). We found a significant enrichment of proteins related to synaptic structure and function among upregulated pathways and a down-regulation of metabolic pathways and mechanisms associated to RNA translation in control females compared to males (Fig. S4; Table S8).

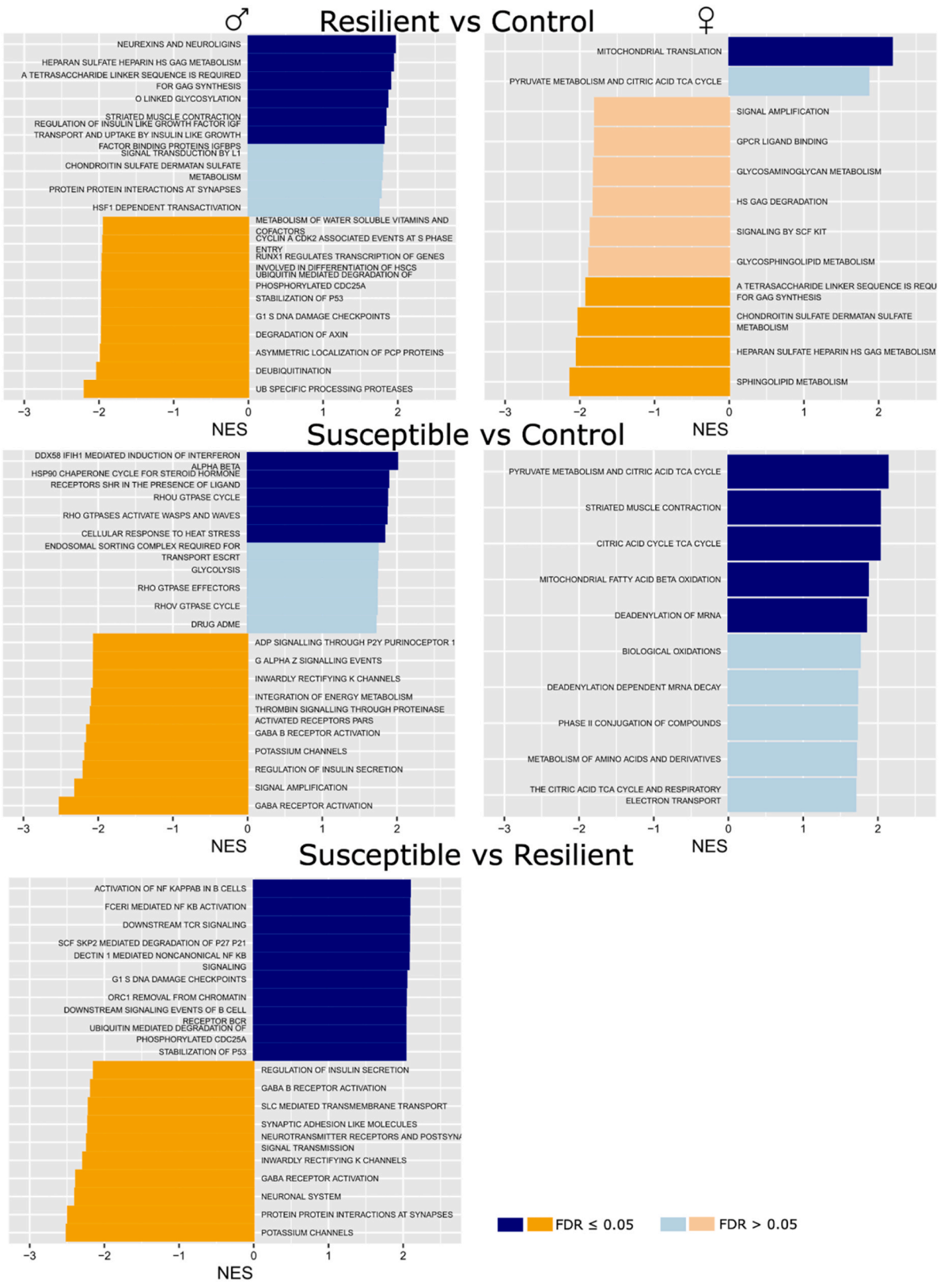

Fig. 6. Gene Set Enrichment Analyses (GSEA) *revealed sex- and susceptibility/resilience-dependent changes of the synaptic proteomic landscape of the hippocampus.* Bar charts depicting the GSEA results. The following comparisons were considered: resilient versus control mice; susceptible versus control mice; susceptible versus resilient mice. All the analyses are reported stratified for sex. Only the top 10 significantly enriched Reactome canonical pathways are reported. The horizontal axis represents the positive (blue) and negative (orange) normalized enrichment scores (NES). The transparency of the bar chart represents the FDR. Pathways with a FDR < 0.05 are reported in dark colours whereas pathways with a FDR < 0.10 are reported in light colors.

Minor changes were found between resilient female and male mice, with the involvement of mitochondrial processes among upregulated pathways and a downregulation of metabolic pathways (Fig. S4; Table S9). More changes were instead found between susceptible female and male mice, with an upregulation of pathways related to synaptic structure and function, and a downregulation of inflammatory pathways (Fig. S4; Table S10). Overall, the direct comparison of male and female mice showed a different synaptoproteome profile at baseline, converging in resilient animals, while further diverging under susceptible conditions.

3.5. Inhibition of Rac1/3 GTPases reversed the hippocampal LTP impairment exclusively in susceptible male mice

As aforementioned, we found several pathways involving RHO Family GTPases upregulated exclusively in susceptible male mice. Among enriched proteins upregulated in these pathways, we found Rac GTPases. Among Rac GTPases, especially Rac1 and Rac3 GTPases play a synergistic role in the regulation of structural and synaptic plasticity in the hippocampus [43], also in relation to traumatic stress response, which was reported to increase Rac GTPases-related signaling pathways [44]. We thus decided to test the hypothesis that inhibition of Rac1/3 GTPases could rescue the hippocampal LTP impairment in a sex-dependent manner. For this purpose, we selected EHop-016, a highly potent and selective Rac 1/3 GTPase inhibitor. The treatment of hippocampal slices with EHop-016 fully rescued hippocampal LTP impairment in susceptible male mice but had no effect in susceptible females (Fig. 7A-C). This suggests a sex-specific contribution of Rac1/3 signaling to the synaptic plasticity impairment induced by traumatic stress. Notably, EHop-016 treatment reduced LTP in control mice of both sexes (Fig. 7A-C), indicating that the fine-tuning of Rac1/3 signaling is required to maintain physiological synaptic plasticity.

4. Discussion

Clinical findings consistently show that women are approximately twice as likely as men to develop PTSD, despite often experiencing fewer traumatic events overall [45,46]. Other clinical studies indicate that women are at higher risk of developing PTSD compared to men because they are more frequently exposed to specific traumatic events carrying greater pathogenicity, such as child sexual abuse [47]. This has been however questioned by other findings reporting higher PTSD vulnerability in women regardless of the trauma type [8]. Women also tend to exhibit more severe PTSD symptoms across different time points after trauma exposure [45]. In spite of these evident sex/gender differences in PTSD, the vast majority of preclinical studies aimed at investigating the pathophysiological mechanisms underlying PTSD have been carried out

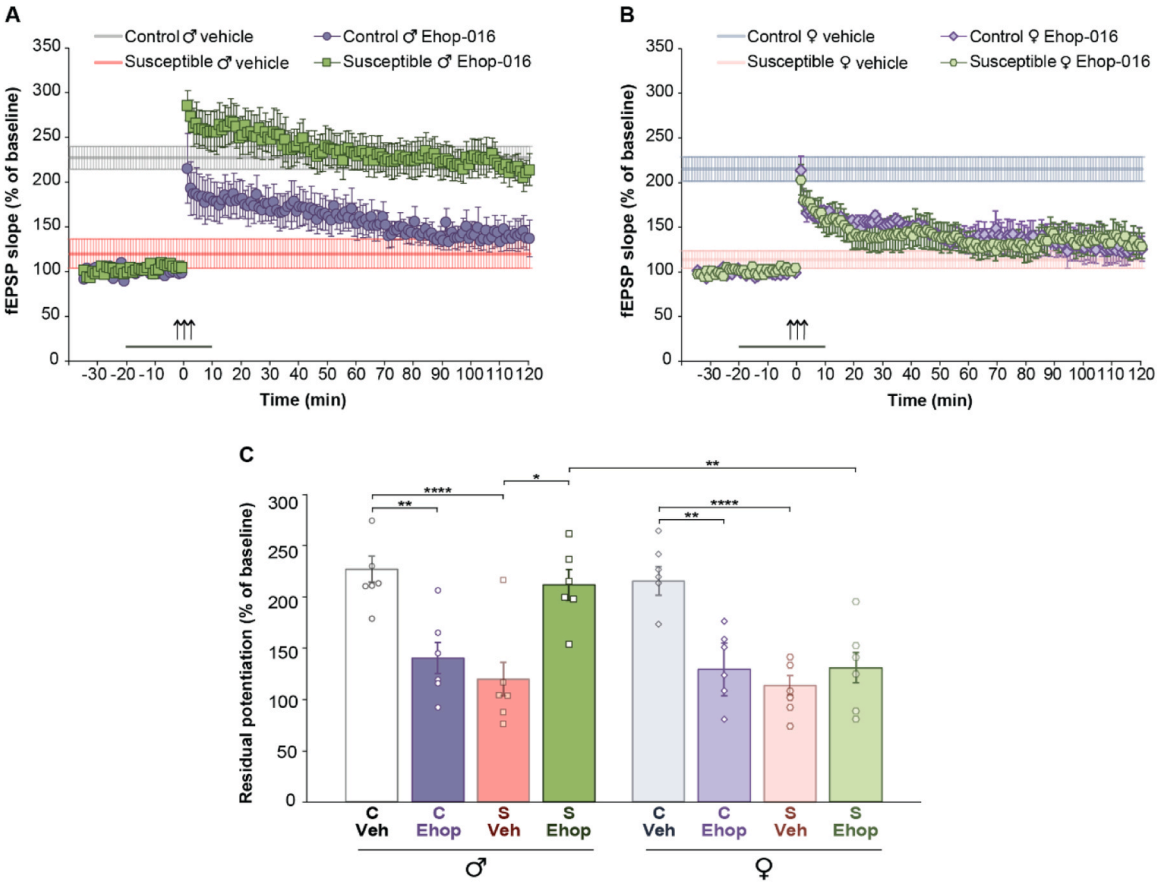

Fig. 7. *EHop-016 rescued the hippocampal LTP impairment in a sex-dependent manner.*(A) The LTP impairment in slices from susceptible male mice was restored by perfusion of hippocampal slices with the Rac1/3 GTPases inhibitor EHop-016 (20 min before + 10 min after tetanus) (n = 6 slices from 4 animals; $F_{(1,12)} = 21.036$, P = 0.001). EHop-016 treatment impaired LTP in control male mice (n = 6 from 4 animals; $F_{(1,11)} = 15.592$, P = 0.002). Shaded area with dashed line = mean ± SEM of the last LTP recording in vehicle-treated slices shown in Fig. 3B. (B) Treatment with EHop-016 did not rescue the LTP deficit in susceptible female mice (n = 6 slices from 4 animals; $F_{(1,12)} = 0.170$, P = 0.688), while impaired LTP in control females (n = 6 slices from 4 animals; $F_{(1,11)} = 19.903$, P = 0.001). Shaded area with dashed line = mean ± SEM of the last LTP recording in vehicle-treated slices shown in Fig. 3C. (C) Analysis of residual potentiation (averaged over the last 5 min of LTP recording, 120 min post-tetanus) confirmed that EHop-016 rescued the LTP impairment exclusively in susceptible male mice ($F_{(7, 46)} = 11.422$, P < 0.0001 among all groups; Bonferroni post-hoc: susceptible vehicle vs susceptible Ehop males P < 0.0001; susceptible vehicle vs susceptible EHop females P > 0.999; susceptible EHop males vs susceptible Ehop females P = 0.009). Two-way for repeated measure ANOVA or One-way ANOVA. Post hoc comparisons were made using the Bonferroni test: *P < 0.05; **P < 0.01; **** P < 0.0001. All values are presented as means ± s.e.m.

mainly in male rodents [9]. In this study, in line with clinical evidence, we demonstrate that in the AIS model female mice are more prone to develop traumatic stress susceptibility than male mice. We also demonstrate that susceptible female mice identified through the AIS model develop robust and persistent fear responses to trauma-related cue, which appear even more pronounced compared to fear responses of susceptible male mice observed in our previous work [13]. Although further investigation is needed, this is translationally relevant because modeling sex differences in PTSD susceptibility and resilience has been proved challenging [11,48,49]. The few studies conducted with female animals have in fact provided contrasting findings that do not broadly reflect the human condition [10,50]. The increased female susceptibility we observed might be due to our individual screening, which is based on trauma-induced changes in startle reactivity. Preclinical findings indeed suggest that females are more susceptible to stress-induced hyperarousal than males [51]. This is in line with human data showing that women are more prone to develop neuropsychiatric disorders characterized by hyperarousal, whereas men are more likely to develop neuropsychiatric disorders characterized by deficits of attention [51].

In line with previous works [52,53], we did not find any significant influence of estrous cycle stage on ASR of susceptible and resilient female mice. These results, together with other findings, suggest that although ovarian hormones are basically key neuromodulators, other factors might be responsible for sex differences in PTSD susceptibility/symptomatology [9].

An impaired hippocampal synaptic plasticity has been consistently linked to the pathophysiology of PTSD [13,21,54]. To the best of our knowledge, here we demonstrate for the first time that a single traumatic event induces long-term hippocampal plasticity deficits exclusively in susceptible mice regardless of sex. Our results support the wide concept that PTSD might be a “synaptic disconnection syndrome” [55]. It is indeed well-established that individuals with PTSD exhibit reduced hippocampal function during memory and fear-related learning tasks, as well as reduced connectivity between the hippocampus and other stress-related brain areas [56]. Importantly, the LTP deficits observed in susceptible mice were not associated with alterations in neurotransmitter release or vesicle recycling, as none of the presynaptic indices of short-term plasticity were affected by trauma. On the other hand, the subtle physiological differences observed in certain forms of synaptic plasticity between control males and females underscore the intrinsic complexity of sex-dependent modulation at the synaptic level. Indeed, recent studies have reported sex differences in presynaptic function, including variations in synaptic vesicle recycling dynamics and glutamate release probability, particularly within hippocampal and striatal circuits [57,58].

Our morphological analysis shows an increased length of CA1 pyramidal neurons apical dendrites as well as higher spine density of basal dendrites in susceptible male but not female mice. These results demonstrate that maladaptive structural plasticity alterations induced by a single traumatic event are sex-dependent and may be different from those induced by chronic stress [59]. These results may also explain the hippocampal LTP deficit we previously observed in male susceptible mice. It has indeed demonstrated that changes in the length of the apical dendrites can affect the pyramidal cells ability to induce burst firing, which is necessary for the induction of LTP [60]. The fact that we did not find maladaptive structural plasticity alterations in the hippocampus of female susceptible mice indicates that more complex mechanisms and dysfunctions of other brain areas foster the development of female traumatic stress susceptibility [9,61]. We remarkably also uncovered adaptive structural plasticity changes of DG granule neurons of exclusively female resilient mice. In this respect, the DG is a subregion of the hippocampus highly involved in shaping stress susceptibility/resilience [62]. Indeed, the anatomical connections between the DG and the amygdala are crucial for processes related to fear-related learning and memory [63]. Our results indicate that further studies are needed to understand sex-dependent DG responses to trauma/stress, also because most of the structural plasticity studies have been conducted using predominantly male mice.

The study of the synaptoproteome can give information about molecular changes occurring at synapses [41]. Our study reveals no significant difference in the expression of single proteins, suggesting no major protein changes at synapses. This suggests that the long-term impact of trauma on synaptic protein expression profiles is modest and lower than the detection power of our study. For this reason, future studies with larger cohorts and analysis at different timepoints are needed. Despite the limited statistical power in detecting associations at the individual protein level, our study was able to identify significant differences in the expression of specific gene-sets with sex- and phenotype-dependent changes. Interestingly, GSEA revealed that the synaptoproteomic profiles of susceptible and resilient female mice exhibited a striking similarity to each other but at the same time are markedly different from those of susceptible and resilient male mice. The enhancement of pathways related to mitochondrial functions suggests an increased metabolic activity in trauma-exposed female mice. These results are in line with a previous study showing that traumatic stress induced sex-specific alterations of mitochondrial function in the synapse, with trauma-exposed female mice more sensitive to long-term functional changes of synaptic mitochondria (increased respiration) [64]. We also observed a significant downregulation of pathways related to sphingolipids metabolism in resilient female mice. This may be a relevant sex-specific resilient mechanism because increased sphingolipids pools produce pathophysiological mechanisms by boosting lipotoxic insults [65]. Notably, GSEA also revealed a downregulation of pathways related to synaptic transmission and plasticity in susceptible male mice, which correlates with the electrophysiological results showing synaptic plasticity deficits. Importantly, the enrichment of proteins belonging to the neurexins and neuroligins pathways suggests that resilient male mice adopt active coping strategies aimed at preserving hippocampal synaptic plasticity processes. Indeed, hypofunction of neurexins was shown to lead to behavioral abnormalities related to neuropsychiatric disorders as well as to synaptic plasticity impairment [66]. Conversely, we found that several pathways involving RHO family GTPases were upregulated exclusively in susceptible male mice. Among these, Rac1 and Rac3 cooperate to regulate actin-dependent remodeling processes that support both structural and functional plasticity in the hippocampus [43]. It is therefore plausible that the upregulation of Rac-dependent pathways contributes to the structural alterations observed in CA1 exclusively in susceptible male mice, which may in turn underlie the LTP impairment. This interpretation is supported by previous findings showing that enhanced Rac1 activity is associated with increased CA1 spine density and concomitant LTP deficits [67,68].

In this study, consistent with evidence from previous studies [44], we uncovered that the Rac 1/3 GTPase inhibitor EHop-016 successfully rescued hippocampal LTP impairment in susceptible male mice. Importantly, EHop-016 did not rescue the hippocampal LTP impairment in susceptible female mice. This sex-specific effect aligns with our molecular data showing that RHO family GTPase pathways were upregulated exclusively in susceptible males, suggesting that Rac1/3 overactivation contributes to LTP impairment only in this group. In contrast, the absence of such molecular alterations in females likely accounts for the inefficacy of EHop-016 and indicates that distinct mechanisms underlie hippocampal synaptic plasticity dysfunction and traumatic stress susceptibility in the two sexes. The differential response to EHop-016 may thus reflect sex-dependent signaling cascades governing hippocampal LTP and the distinct ways in which traumatic stress affects synaptic structure and function. NMDA receptors are key mediators of Rac1 GTPase activation, which is crucial for the synaptic remodeling that fosters the induction and maintenance of LTP [69]. Our findings suggest that traumatic stress-induced aberrant NMDA receptor activation [70] could lead to Rac GTPase signaling overactivation, thereby contributing to the LTP impairment we found in susceptible male mice. EHop-016 can effectively normalize this dysregulation by

potently inhibiting Rac1 and Rac3 GTPases. This normalization would then restore NMDAR-dependent LTP, thereby rescuing the synaptic plasticity deficits. Conversely, the inefficacy of EHop-016 in susceptible female mice indicates that traumatic stress induces hippocampal LTP deficits via distinct Rac1/3-independent mechanisms, which warrant further experimental investigation to be fully elucidated. Overall, this suggests profound sex-dependent differences in the pathophysiology of stress-related disorders including PTSD. The differential efficacy of EHop-016 supports the rationale for sex-specific approaches in developing effective pharmacotherapies for PTSD. It is also important to underline that in line with other studies [71], EHop-016 induced LTP impairment in control mice of both sexes. This implies that the maintenance of an optimal range of Rac 1/3 GTPase activity is pivotal for proper hippocampal synaptic function.

In conclusion, our study indicates that the mechanisms underlying resilience and susceptibility to trauma are robustly driven by sex. Effective and targeted pharmacological treatments for PTSD may be developed by studying sex-dependent pathophysiological mechanisms, which may ultimately lead to sex-tailored therapeutic interventions.

CRediT authorship contribution statement

Clizia Chinello: Methodology, Investigation. **Jessica Mingardi:** Methodology, Investigation. **Gian Marco Leggio:** Writing – review & editing, Writing – original draft, Validation, Supervision, Project administration, Investigation, Funding acquisition, Conceptualization. **Alessandro Barbon:** Methodology, Investigation. **Laura Musazzi:** Writing – review & editing, Writing – original draft, Validation, Investigation, Conceptualization. **Chiara Magri:** Methodology, Investigation. **Loredana Leggio:** Methodology, Investigation. **Isabella Piga:** Methodology, Investigation. **Lisa Pagani:** Methodology, Investigation. **Daniela Puzzo:** Methodology, Investigation. **Mattia Giovenzana:** Methodology, Investigation. **Filippo Drago:** Supervision. **Silvia Rizzo:** Methodology, Investigation. **Walter Gulisano:** Validation, Software, Methodology, Investigation. **Maria Rosaria Tropea:** Validation, Software, Methodology, Investigation. **Nunzio Iraci:** Methodology, Investigation. **Torrisi Sebastiano Alfio:** Writing – review & editing, Writing – original draft, Validation, Methodology, Investigation, Formal analysis, Data curation, Conceptualization.

Funding

This work was supported by the Italian Ministry of Health, PNRR-MAD-2022–12376156 to G.M.L and University of Milano-Bicocca (FAQC 2021–3) intramural funds to LM.

Declaration of generative AI and AI-assisted technologies in the writing process

During the preparation of this work the authors used ChatGPT Model 4 in the writing process to correct grammatical errors and improve readability of this manuscript. After using this tool, the authors reviewed and edited the content as needed and take full responsibility for the content of the published article.

Declaration of Competing Interest

The authors declare the following financial interests/personal relationships which may be considered as potential competing interests: Gian Marco Leggio reports financial support was provided by Italian Ministry of Health. Laura Musazzi reports financial support and administrative support were provided by University of Milano-Bicocca. If there are other authors, they declare that they have no known competing financial interests or personal relationships that could have appeared to influence the work reported in this paper.

Acknowledgments

We thank M. Abbate, G. Barbera, E. Giuffrida, G. Valastro, N. Pulvirenti, and C. Paoli for technical support.

Appendix A. Supporting information

Supplementary data associated with this article can be found in the online version at doi:10.1016/j.phrs.2025.108072.

Data availability

Data will be made available on request.

References

[1] K.J. Ressler, S. Berretta, V.Y. Bolshakov, I.M. Rosso, E.G. Meloni, S.L. Rauch, W. A. Carlezon Jr., Post-traumatic stress disorder: clinical and translational neuroscience from cells to circuits, Nat. Rev. Neurol. 18 (2022) 273–288.
[2] G. Richter-Levin, O. Stork, M.V. Schmidt, Animal models of PTSD: a challenge to be met, Mol. Psychiatry 24 (2019) 1135–1156.
[3] L.E. Watkins, K.R. Sprang, B.O. Rothbaum, Treating PTSD: a review of evidence-based psychotherapy interventions, Front Behav. Neurosci. 12 (2018) 258.
[4] C. Schrader, A. Ross, A review of PTSD and current treatment strategies, Mo Med 118 (2021) 546–551.
[5] S.A. Torrisi, G.M. Leggio, F. Drago, S. Salomone, Therapeutic challenges of post-traumatic stress disorder: focus on the dopaminergic system, Front. Pharm. 10 (2019) 404.
[6] D.N. Ditlevsen, A. Elklit, Gender, trauma type, and PTSD prevalence: a re-analysis of 18 nordic convenience samples, Ann. Gen. Psychiatry 11 (2012) 26.
[7] R.C. Kessler, A. Sonnega, E. Bromet, M. Hughes, C.B. Nelson, Posttraumatic stress disorder in the National Comorbidity Survey, Arch. Gen. Psychiatry 52 (1995) 1048–1060.
[8] T.S. Ramikie, K.J. Ressler, Mechanisms of Sex Differences in Fear and Posttraumatic Stress Disorder, Biol. Psychiatry 83 (2018) 876–885.
[9] R.M. Shansky, A.Z. Murphy, Considering sex as a biological variable will require a global shift in science culture, Nat. Neurosci. 24 (2021) 457–464.
[10] R.M. Shansky, Sex differences in PTSD resilience and susceptibility: challenges for animal models of fear learning, Neurobiol. Stress 1 (2015) 60–65.
[11] H. Cohen, R. Yehuda, Gender differences in animal models of posttraumatic stress disorder, Dis. Markers 30 (2011) 141–150.
[12] N. Kokras, C. Dalla, Sex differences in animal models of psychiatric disorders, Br. J. Pharm. 171 (2014) 4595–4619.
[13] S.A. Torrisi, G. Lavanco, O.M. Maurel, W. Gulisano, S. Laudani, F. Geraci, M. Grasso, C. Barbagallo, F. Caraci, C. Bucolo, M. Ragusa, F. Papaleo, P. Campolongo, D. Puzzo, F. Drago, S. Salomone, G.M. Leggio, A novel arousal-based individual screening reveals susceptibility and resilience to PTSD-like phenotypes in mice, Neurobiol. Stress 14 (2021) 100286.
[14] X. Chu, Y. Zhou, Z. Hu, J. Lou, W. Song, J. Li, X. Liang, C. Chen, S. Wang, B. Yang, L. Chen, X. Zhang, J. Song, Y. Dong, S. Chen, L. He, Q. Xie, X. Chen, W. Li, 24-hour-restraint stress induces long-term depressive-like phenotypes in mice, Sci. Rep. 6 (2016) 32935.
[15] O.M. Maurel, S.A. Torrisi, C. Barbagallo, M. Purrello, S. Salomone, F. Drago, M. Ragusa, G.M. Leggio, Dysregulation of miR-15a-5p, miR-497a-5p and miR-511-5p Is Associated with Modulation of BDNF and FKBP5 in Brain Areas of PTSD-Related Susceptible and Resilient Mice, Int J. Mol. Sci. 22 (2021).
[16] S. Laudani, S.A. Torrisi, S. Alboni, T.F.S. Bastiaanssen, C. Benatti, V. Rivi, R. D. Moloney, V. Fuochi, P.M. Furneri, F. Drago, S. Salomone, F. Tascedda, J. F. Cryan, G.M. Leggio, Gut microbiota alterations promote traumatic stress susceptibility associated with p-cresol-induced dopaminergic dysfunctions, Brain Behav. Immun. 107 (2023) 385–396.
[17] L.M. Shin, S.L. Rauch, R.K. Pitman, Amygdala, medial prefrontal cortex, and hippocampal function in PTSD, Ann. N. Y Acad. Sci. 1071 (2006) 67–79.
[18] X.L. Bian, C. Qin, C.Y. Cai, Y. Zhou, Y. Tao, Y.H. Lin, H.Y. Wu, L. Chang, C.X. Luo, D.Y. Zhu, Anterior cingulate cortex to ventral hippocampus circuit mediates contextual fear generalization, J. Neurosci. 39 (2019) 5728–5739.
[19] I. Izquierdo, C.R. Furini, J.C. Myskiw, Fear Memory, Physiol. Rev. 96 (2016) 695–750.
[20] J.L. McGaugh, The amygdala modulates the consolidation of memories of emotionally arousing experiences, Annu Rev. Neurosci. 27 (2004) 1–28.
[21] Y. Du, Y. Li, X. Zhao, Y. Yao, B. Wang, L. Zhang, G. Wang, Psilocybin facilitates fear extinction in mice by promoting hippocampal neuroplasticity, Chin. Med J. (Engl.) 136 (2023) 2983–2992.
[22] M. He, J.X. Wei, M. Mao, G.Y. Zhao, J.J. Tang, S. Feng, X.M. Lu, Y.T. Wang, Synaptic Plasticity in PTSD and associated Comorbidities: The Function and Mechanism for Diagnostics and Therapy, Curr. Pharm. Des. 24 (2018) 4051–4059.
[23] B.L. Montalvo-Ortiz, L. Castillo-Pichardo, E. Hernandez, T. Humphries-Bickley, A. De la Mota-Peynado, L.A. Cubano, C.P. Vlaar, S. Dharmawardhane, Characterization of EHop-016, novel small molecule inhibitor of Rac GTPase, J. Biol. Chem. 287 (2012) 13228–13238.

[24] V.G. Olson, H.R. Rockett, R.K. Reh, V.A. Redila, P.M. Tran, H.A. Venkov, M. C. Defino, C. Hague, E.R. Peskind, P. Szot, M.A. Raskind, The role of norepinephrine in differential response to stress in an animal model of posttraumatic stress disorder, Biol. Psychiatry 70 (2011) 441–448.
[25] J.P. Guilloux, M. Seney, N. Edgar, E. Sibille, Integrated behavioral z-scoring increases the sensitivity and reliability of behavioral phenotyping in mice: relevance to emotionality and sex, J. Neurosci. Methods 197 (2011) 21–31.
[26] C.S. Caligioni, Assessing reproductive status/stages in mice, Curr. Protoc. Neurosci. Append. 4 (2009). Appendix 4I.
[27] M.C. Cora, L. Kooistra, G. Travlos, Vaginal Cytology of the Laboratory Rat and Mouse: Review and Criteria for the Staging of the Estrous Cycle Using Stained Vaginal Smears, Toxicol. Pathol. 43 (2015) 776–793.
[28] M.R. Tropea, D.D. Li Puma, M. Melone, W. Gulisano, O. Arancio, C. Grassi, F. Conti, D. Puzzo, Genetic deletion of alpha7 nicotinic acetylcholine receptors induces an age-dependent Alzheimer's disease-like pathology, Prog. Neurobiol. 206 (2021) 102154.
[29] J. Mingardi, E. Ndoj, T. Bonifacino, P. Misztak, M. Bertoli, L. La Via, C. Torazza, I. Russo, M. Milanese, G. Bonanno, M. Popoli, A. Barbon, L. Musazzi, Functional and Molecular Changes in the Prefrontal Cortex of the Chronic Mild Stress Rat Model of Depression and Modulation by Acute Ketamine, Int J. Mol. Sci. 24 (2023).
[30] P. Previtali, L. Pagani, G. Risca, G. Capitoli, E. Bossi, G. Oliveira, I. Piga, A. Radice, B. Trezzi, R.A. Sinico, F. Magni, C. Chinello, Towards the definition of the molecular hallmarks of idiopathic membranous nephropathy in serum proteome: a DIA-PASEF approach, Int J. Mol. Sci. 24 (2023).
[31] Y. Zhu, L.M. Orre, Y. Zhou Tran, G. Mermelekas, H.J. Johansson, A. Malyutina, S. Anders, J. Lehtio, DEqMS: a method for accurate variance estimation in differential protein expression analysis, Mol. Cell Proteom. 19 (2020) 1047–1057.
[32] G.K. Smyth, Linear models and empirical bayes methods for assessing differential expression in microarray experiments, Stat. Appl. Genet Mol. Biol. 3 (2004). Article3.
[33] Y. Liao, J. Wang, E.J. Jaehnig, Z. Shi, B. Zhang, WebGestalt 2019: gene set analysis toolkit with revamped UIs and APIs, Nucleic Acids Res 47 (2019) W199–W205.
[34] T. Bonifacino, J. Mingardi, R. Facchinetti, N. Sala, G. Frumento, E. Ndoj, M. Valenza, C. Paoli, A. Ieraci, C. Torazza, M. Balbi, M. Guerinoni, N. Muhammad, I. Russo, M. Milanese, C. Scuderi, A. Barbon, L. Steardo, G. Bonanno, M. Popoli, L. Musazzi, Changes at glutamate tripartite synapses in the prefrontal cortex of a new animal model of resilience/vulnerability to acute stress, Transl. Psychiatry 13 (2023) 62.
[35] N. Sala, C. Paoli, T. Bonifacino, J. Mingardi, E. Schiavon, L. La Via, M. Milanese, P. Tornese, A.K. Datusalia, J. Rosa, R. Facchinetti, G. Frumento, G. Carini, F. Salerno Scarzella, C. Scuderi, L. Forti, A. Barbon, G. Bonanno, M. Popoli, L. Musazzi, Acute Ketamine Facilitates Fear Memory Extinction in a Rat Model of PTSD Along With Restoring Glutamatergic Alterations and Dendritic Atrophy in the Prefrontal Cortex, Front Pharm. 13 (2022) 759626.
[36] S. Preibisch, S. Saalfeld, P. Tomancak, Globally optimal stitching of tiled 3D microscopic image acquisitions, Bioinformatics 25 (2009) 1463–1465.
[37] M.H. Longair, D.A. Baker, J.D. Armstrong, Simple Neurite Tracer: open source software for reconstruction, visualization and analysis of neuronal processes, Bioinformatics 27 (2011) 2453–2454.
[38] C. Arshadi, U. Gunther, M. Eddison, K.I.S. Harrington, T.A. Ferreira, SNT: a unifying toolbox for quantification of neuronal anatomy, Nat. Methods 18 (2021) 374–377.
[39] M.A. Lynch, Long-term potentiation and memory, Physiol. Rev. 84 (2004) 87–136.
[40] Y. Yang, X.B. Wang, M. Frerking, Q. Zhou, Spine expansion and stabilization associated with long-term potentiation, J. Neurosci. 28 (2008) 5740–5751.
[41] F. Bai, F.A. Witzmann, Synaptosome proteomics, Subcell. Biochem 43 (2007) 77–98.
[42] T.C. Sudhof, Neuroligins and neurexins link synaptic function to cognitive disease, Nature 455 (2008) 903–911.
[43] R. Pennucci, I. Gucciardi, I. de Curtis, Rac1 and Rac3 GTPases differently influence the morphological maturation of dendritic spines in hippocampal neurons, PLoS One 14 (2019) e0220496.
[44] S. Yang, J. Hu, Y. Chen, Z. Zhang, J. Wang, G. Zhu, DCC, a potential target for controlling fear memory extinction and hippocampal LTP in male mice receiving single prolonged stress, Neurobiol. Stress 32 (2024) 100666.
[45] L.A. Irish, B. Fischer, W. Fallon, E. Spoonster, E.M. Sledjeski, D.L. Delahanty, Gender differences in PTSD symptoms: an exploration of peritraumatic mechanisms, J. Anxiety Disord. 25 (2011) 209–216.
[46] L. Ronning, R.L. Zelkowitz, M.L. Piccirillo, J. Liu, J.L. Thomas, J. Guler, J.J. Kyei, C.M. Hoeboer, J.F. Karchoud, M. Olff, A.B. Witteveen, M. van Zuiden, Gender differences in early posttraumatic stress disorder symptoms: a network analysis, Eur. J. Psychotraumatol. 16 (2025) 2448385.
[47] D.F. Tolin, E.B. Foa, Sex differences in trauma and posttraumatic stress disorder: a quantitative review of 25 years of research, Psychol. Bull. 132 (2006) 959–992.
[48] E.P. Bauer, Sex differences in fear responses: Neural circuits, Neuropharmacology 222 (2023) 109298.
[49] G.F. Mancini, S.A. Torrisi, E.M.G. Viho, O.C. Meijer, G.M. Leggio, P. Campolongo, Interindividual and sex differences in resilience and vulnerability to post-traumatic stress disorder (PTSD): insights from animal models, Biol. Sex. Differ. 16 (2025) 50.
[50] S.T. Gonzalez, V. Marty, I. Spigelman, S.P. Reise, M.S. Fanselow, Impact of stress resilience and susceptibility on fear learning, anxiety, and alcohol intake, Neurobiol. Stress 15 (2021) 100335.
[51] D.A. Bangasser, S.R. Eck, E.Ordones Sanchez, Sex differences in stress reactivity in arousal and attention systems, Neuropsychopharmacology 44 (2019) 129–139.
[52] A. Mazor, M.A. Matar, Z. Kaplan, N. Kozlovsky, J. Zohar, H. Cohen, Gender-related qualitative differences in baseline and post-stress anxiety responses are not reflected in the incidence of criterion-based PTSD-like behaviour patterns, World J. Biol. Psychiatry 10 (2009) 856–869.
[53] Y. Zhao, E.Y. Bijlsma, M.P. Verdouw, L. Groenink, No effect of sex and estrous cycle on the fear potentiated startle response in rats, Behav. Brain Res 351 (2018) 24–33.
[54] W. Niu, Y. Duan, Y. Kang, X. Cao, Q. Xue, Propofol improves learning and memory in post-traumatic stress disorder (PTSD) mice via recovering hippocampus synaptic plasticity, Life Sci. 293 (2022) 120349.
[55] J.H. Krystal, C.G. Abdallah, L.A. Averill, B. Kelmendi, I. Harpaz-Rotem, G. Sanacora, S.M. Southwick, R.S. Duman, Synaptic Loss and the Pathophysiology of PTSD: Implications for Ketamine as a Prototype Novel Therapeutic, Curr. Psychiatry Rep. 19 (2017) 74.
[56] S.A. Joshi, E.R. Duval, B. Kubat, I. Liberzon, A review of hippocampal activation in post-traumatic stress disorder, Psychophysiology 57 (2020) e13357.
[57] M.C. Knouse, A.U. Deutschmann, M.N. Nenov, M.E. Wimmer, L.A. Briand, Sex differences in pre- and post-synaptic glutamate signaling in the nucleus accumbens core, Biol. Sex. Differ. 14 (2023) 52.
[58] S.M. Sertel, W. Blumenstein, S. Mandad, O. Shomroni, G. Salinas, S.O. Rizzoli, Differences in synaptic vesicle pool behavior between male and female hippocampal cultured neurons, Sci. Rep. 11 (2021) 17374.
[59] B.S. McEwen, C. Nasca, J.D. Gray, Stress Effects on Neuronal Structure: Hippocampus, Amygdala, and Prefrontal Cortex, Neuropsychopharmacology 41 (2016) 3–23.
[60] R.A. van Elburg, A. van Ooyen, Impact of dendritic size and dendritic topology on burst firing in pyramidal cells, PLoS Comput. Biol. 6 (2010) e1000781.
[61] L.A. Galea, B.S. McEwen, P. Tanapat, T. Deak, R.L. Spencer, F.S. Dhabhar, Sex differences in dendritic atrophy of CA3 pyramidal neurons in response to chronic restraint stress, Neuroscience 81 (1997) 689–697.
[62] A. Besnard, A. Sahay, Adult Hippocampal Neurogenesis, Fear Generalization, and Stress, Neuropsychopharmacology 41 (2016) 24–44.
[63] B.S. McEwen, Stress, sex, and neural adaptation to a changing environment: mechanisms of neuronal remodeling, Ann. N. Y Acad. Sci. 1204 (2010) E38–E59.
[64] G.A. Shaw, M.M. Hyer, I. Targett, K.R. Council, S.K. Dyer, S. Turkson, C.M. Burns, G.N. Neigh, Traumatic stress history interacts with sex and chronic peripheral inflammation to alter mitochondrial function of synaptosomes, Brain Behav. Immun. 88 (2020) 203–219.
[65] S. Rodriguez-Cuenca, V. Pellegrinelli, M. Campbell, M. Oresic, A. Vidal-Puig, Sphingolipids and glycerophospholipids - The "ying and yang" of lipotoxicity in metabolic diseases, Prog. Lipid Res 66 (2017) 14–29.
[66] E. Kasem, T. Kurihara, K. Tabuchi, Neurexins and neuropsychiatric disorders, Neurosci. Res 127 (2018) 53–60.
[67] D. Oh, S. Han, J. Seo, J.R. Lee, J. Choi, J. Groffen, K. Kim, Y.S. Cho, H.S. Choi, H. Shin, J. Woo, H. Won, S.K. Park, S.Y. Kim, J. Jo, D.J. Whitcomb, K. Cho, H. Kim, Y.C. Bae, N. Heisterkamp, S.Y. Choi, E. Kim, Regulation of synaptic Rac1 activity, long-term potentiation maintenance, and learning and memory by BCR and ABR Rac GTPase-activating proteins, J. Neurosci. 30 (2010) 14134–14144.
[68] H. Zhang, Y. Ben Zablah, H. Zhang, Z. Jia, Rho Signaling in Synaptic Plasticity, Memory, and Brain Disorders, Front Cell Dev. Biol. 9 (2021) 729076.
[69] K.F. Tolias, J.B. Bikoff, A. Burette, S. Paradis, D. Harrar, S. Tavazoie, R. J. Weinberg, M.E. Greenberg, The Rac1-GEF Tiam1 couples the NMDA receptor to the activity-dependent development of dendritic arbors and spines, Neuron 45 (2005) 525–538.
[70] G. Sanacora, Z. Yan, M. Popoli, The stressed synapse 2.0: pathophysiological mechanisms in stress-related neuropsychiatric disorders, Nat. Rev. Neurosci. 23 (2022) 86–103.
[71] L.A. Martinez, M.V. Tejada-Simon, Pharmacological inactivation of the small GTPase Rac1 impairs long-term plasticity in the mouse hippocampus, Neuropharmacology 61 (2011) 305–312.